T.R.
GEBZE TECHNICAL UNIVERSITY
GRADUATE SCHOOL OF NATURAL AND APPLIED SCIENCES

MINICHANNEL EVAPORATOR DESIGN FOR HEAT TRANSFER ENHANCEMENT IN COMPUTER COOLING APPLICATIONS

MEHMET HARUN SÖKÜCÜ
A THESIS SUBMITTED FOR THE DEGREEE OF
MASTER OF SCIENCE
DEPARTMENT OF MECHANICAL ENGINEERING

GEBZE
2020

T.R.

GEBZE TECHNICAL UNIVERSITY

GRADUATE SCHOOL OF NATURAL AND APPLIED SCIENCES

MINICHANNEL EVAPORATOR DESIGN FOR HEAT TRANSFER ENHANCEMENT IN COMPUTER COOLING APPLICATIONS

MEHMET HARUN SÖKÜCÜ

A THESIS SUBMITTED FOR THE DEGREEE OF

MASTER OF SCIENCE

DEPARTMENT OF MECHANICAL ENGINEERING

THESIS SUPERVISOR

PROF. DR. İLYAS KANDEMİR

GEBZE

2020

T.C.
GEBZE TEKNİK ÜNİVERSİTESİ
FEN BİLİMLERİ ENSTİTÜSÜ

BİLGİSAYAR SOĞUTMA UYGULAMALARI İÇİN MİNİKANALLI EVAPORATOR TASARIMI

MEHMET HARUN SÖKÜCÜ

YÜKSEK LİSANS TEZİ
MAKİNE MÜHENDİSLİĞİ ANABİLİM DALI

DANIŞMANI
PROF. DR. İLYAS KANDEMİR

GEBZE
2020

GEBZE TEKNİK ÜNİVERSİTESİ	**YÜKSEK LİSANS JÜRİ ONAY FORMU**

GTÜ Fen Bilimleri Enstitüsü Yönetim Kurulu'nun 29/01/2020 tarih ve 2020/07 sayılı kararıyla oluşturulan jüri tarafından 15/05/2020 tarihinde tez savunma sınavı yapılan Mehmet Harun SÖKÜCÜ' nün tez çalışması Makine Mühendisliği Anabilim Dalında YÜKSEK LİSANS tezi olarak kabul edilmiştir.

JÜRİ

ÜYE
(TEZ DANIŞMANI) : PROF. DR. İLYAS KANDEMİR

ÜYE : PROF. DR. ALP ER ŞEVKİ KONUKMAN

ÜYE : DR. ÖĞR. ÜYESİ MEHMED RAFET ÖZDEMİR

ONAY

Gebze Teknik Üniversitesi Fen Bilimleri Enstitüsü Yönetim Kurulu'nun

...../...../..... tarih ve ...../..... sayılı kararı.

SUMMARY

In parallel with the developments in electronic component production the heat dissipation amount of the chips has increased considerably. Electronics cooling is one of the most critical concerns in reliable operation of computers. Conventionally, some applications available for electronics cooling such as radiation, free convection, force air - liquid cooling and evaporation. Especially the cooling methods used for military applications and supercomputers needs to be specially designed to supply for electronic components reliable temperatures. Conventional cooling methods for electronic components may be inadequate in harsh operating environments. At this point, active cooling techniques may be considered such as vapor compression refrigeration (VCR) system. In this study, a vapor compression refrigeration system for computers which need to high cooling applications have been studied for maintain the chip surface temperature below the study aim at 85 ^{o}C. At the same time a calculation module, for evaporator optimization and design, has been developed. The minichannel evaporator designs were calculated by selecting from heat transfer and pressure drop equations in literature. Then, the electronic chips, which have 100 - 500 W heat power were modeled experimentally in the test apparatus which was formed by producing the designed evaporators. Chip surface temperatures were measured according to constant evaporation temperature and variable heat power capacity and the results were compared with the generated calculation module.

Key Words: Electronic Cooling, Evaporator, Heat Exchanger, Minichannel, VCR System

ÖZET

Elektronik bileşenlerin üretimindeki gelişmelere paralel olarak çiplerin ısı yayılım miktarı da önemli ölçüde artmıştır. Elektronik soğutma, bilgisayarların güvenilir şekilde çalışmasında en kritik konulardan biridir. Geleneksel olarak, serbest taşınım, zorlanmış hava - sıvı soğutma ve buharlaştırıcı yöntemleri ile elektronik soğutma için bazı uygulamalar mevcuttur. Özellikle askeri uygulamalar ve süper bilgisayarlar için kullanılan soğutma yöntemlerinin, elektronik bileşenlere güvenilir sıcaklıkları sağlamak için özel olarak tasarlanması gerekmektedir. Bu gibi zorlu çalışma ortamlarında elektronik bileşenler için geleneksel soğutma yöntemleri yetersiz kalabilmektedir. Bu durumda, buhar sıkıştırmalı soğutma sistemi aktif bir soğutma sitemi kullanımı tercih edilmektedir. Bu çalışmada, elektronik çiplerin yüzey sıcaklığını 85 ^{o}C olan kritik değerin altında tutmak için buhar sıkıştırmalı soğutma sisteminde kullanılan buharlaştırıcı tasarımı incelenmiştir. Aynı zamanda evaporatör optimizasyonu ve tasarımı için bir hesaplama modülü geliştirilmiştir. Minikanallı buharlaştırıcı tasarımlarında literatürde bulunan ısı transferi ve basınç kaybı denklemleri arasından seçilerek kullanılmıştır. Daha sonra, 100 - 500 W ısı gücüne sahip olan elektronik çipler modellenerek, tasarlanan buharlaştırıcılar için test düzeneğinde deneysel olarak incelenmiştir. Elektronik çiplerin yüzey sıcaklıkları sabit buharlaşma sıcaklığı ve farklı ısıl yüklerde ölçülmüş ve sonuçlar hesaplama modülü ile karşılaştırılmıştır.

Anahtar Kelimeler: Buharlaştırıcı, Buhar Sıkıştırmalı Soğutma Sistemi Elektronik Soğutma, Isı Değiştirici, Minikanal

ACKNOWLEDGEMENTS

I wish to express my sincere gratitude to my supervisor, Assoc. Prof. Dr. Mustafa Fazıl SERİNCAN and Assoc. Prof. Dr. İlyas KANDEMİR for his supports in scope of this study.

I would like to firstly appreciated to Friterm Inc. General Manager Naci ŞAHİN and R&D Manager Dr. Hüseyin ONBAŞIOĞLU and finally my laboratory technicians Yüksel ALTUNKIRAN and Aydın KARABABA for great helping during experiments.

I express my deepest gratitude to Prof. Dr. Feridun ÖZGÜÇ who is great teacher and human, for supports at each stage of my thesis, and I would like to thank my friend and colleague Işıl ÜNAL for biggest helping.

TABLE of CONTENTS

LIST of ABBREVATIONS and ACRONYMS

Abbreviations and Acronyms		Explanations
v	:	Vapor
l	:	Liquid
ζ	:	Friction Coefficient
Δ	:	Difference Gradient
ρ	:	Density
c_p	:	Heat Capacity (Constant Pressure)
μ	:	Dynamic Viscosity
k	:	Thermal Conductivity
h	:	Enthalpy
k_s	:	Pipe Roughness
Re	:	Reynolds Number
Pr	:	Prandtl Number
Nu	:	Nusselt Number
Co	:	Convection Number
Fr	:	Froud Number
Bo	:	Boiling Number
m	:	Mass Flow
q	:	Total Heat (From Chips)
G	:	Mass Flux
D_{in}	:	Tube Diameter
L_{tube}	:	Tube Length
E_L	:	Evaporator Length
N_{tube}	:	Number of Tube
D_{maj}	:	Tube Major Diameter
D_{min}	:	Tube Minor Diameter
t_{tube}	:	Tube Wall Thickness
C_W	:	Channel Width

NC	:	Number of Channels in Tube
NCT	:	Total Number of Tubes
C_H	:	Channel Height
D_H	:	Hydraulic Diameter
β	:	Aspect Ratio of Channel
$A_{tubebare}$	:	Outside Tube Area
A_{inside}	:	Effective Surface Area for Heat Transfer
$A_{tubecrossreal}$	:	Flow Cross Section Area
A_{tubeDh}	:	Flow Cross Section Area Based on Hydraulic Diameter
SBS	:	Step By Step
HTC	:	Heat Transfer Coefficient
TP	:	Two Phase
SP	:	Single Phase
CC	:	Correction Coefficient
max	:	Maximum
CPU	:	Central Processing Unit
COP	:	The Coefficient of Performance
VCR	:	Vapor Compression Refrigeration
ODP	:	Ozone Deplation Potential
GWP	:	Global Warming Potential

LIST of FIGURES

LIST of TABLES

1. INTRODUCTION

The development in many areas such as technology, communication, computers, military vehicles are the miniaturization of electronic components and the increasing number of chip per unit area. Miniaturization of electronic components have been resulted 50-1.000 components per chip in the 1960s, 1.000-100.000 components in the 1970s, and 10.000.000 components per chip the end of the 1980s. While 32-bit processors had 3.1 million transistors in the 1990s, super-powered 10-core Xeon processors with 5.5 million transistors, 100 million transistors per square centimeter, were produced in 2006. At this rate, it is estimated that by the end of 2020, the transistor sizes will be reduced to 6 nanometers and the density of 20 billion transistors per cm^2 will be reached. This development also leads to high power densities and high operating temperatures and low performance and long life of electronic devices [1]-[4].

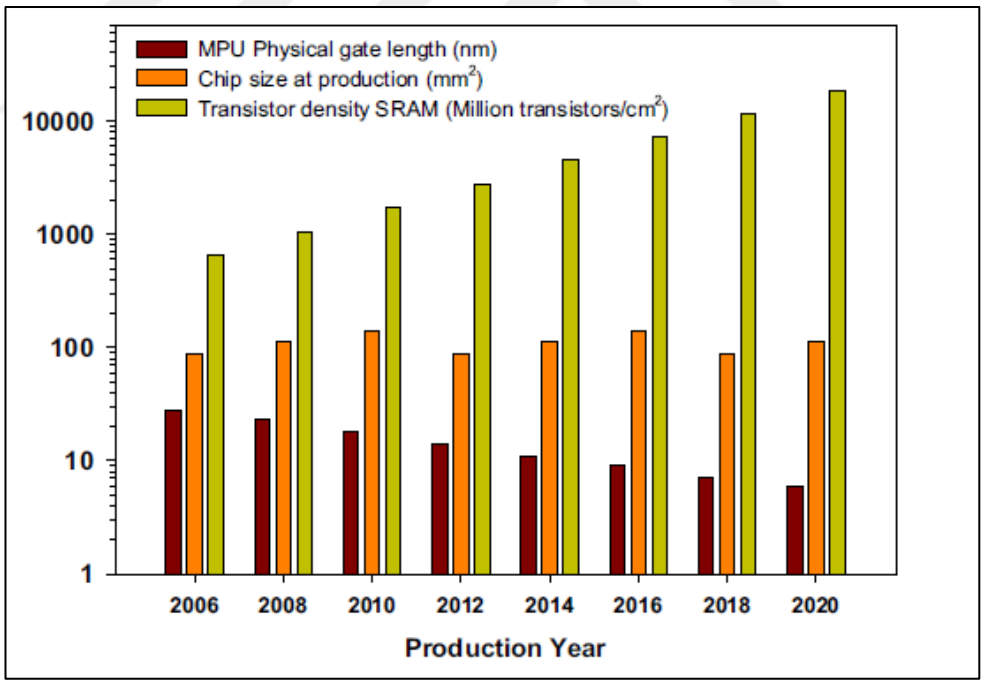

Figure 1.1: Transistor density, chip size and physical gate length of high performance microprocessor chips.

The maximum power dissipation and heat flux from the high performance chips are assumed to increase 360 W and 190 W/cm^2, by 2020 [5].

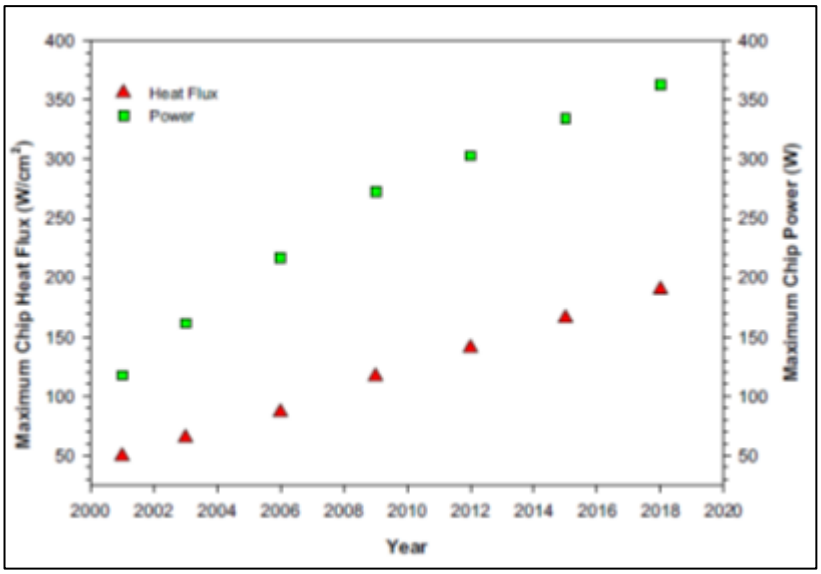

Figure 1.2: Projections of maximum heat flux and power dissipation for microprocessor chips.

Accordingly a study at 2007 [6], many micro- and power-electronics is difficult challenge of removing very high heat flux around 300 W/cm^2 by the time maintaining the temperature below 85 °C. The failure rate of electronic devices increases fault with increasing the operating temperature. The failure factor, which is relative failure rate at any temperature over failure rate at 75 °C, increases exponentially with increasing the device temperature as shown in Figure 1.3 [7-8].

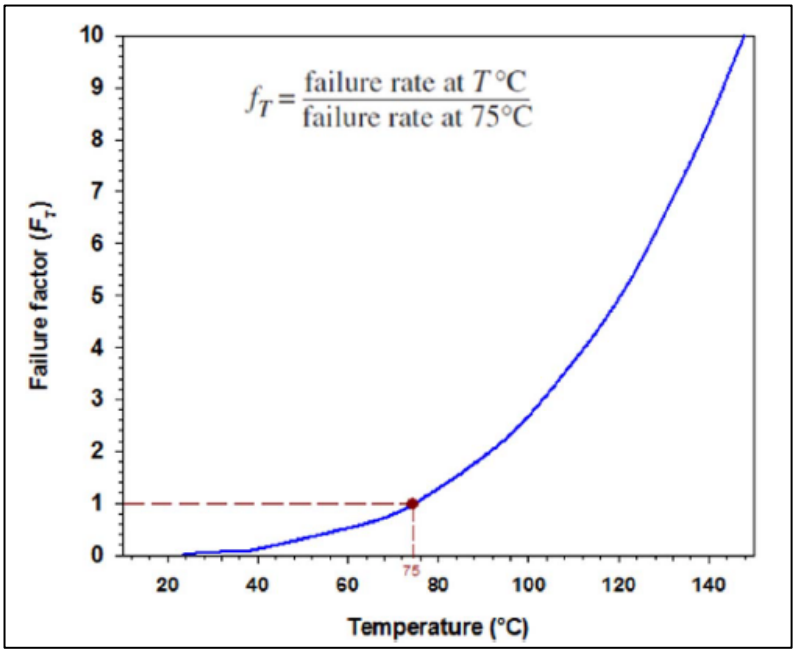

Figure 1.3: Temperature dependence of failure rate of digital devices.

Chips and semiconductors are not used alone. In systems, these electronic components are brought together and used according to need. This process is called electronic packaging. Electronic systems can be packaged as a portable device or a device adapted to be permanently fixed to the rack. Different design criteria can be applied in electronic packaging for aviation, marine and military systems.

This packaging process electronic components; supply protection against mechanical damage, overheating, noise emission and electrostatic discharge. In the case of electronic packaging, the electronic components must be brought together in particular, paying particular attention to the heat transfer mechanism.

Electronics Packaging Levels [9]; Electronic packaging is made according to the levels.

- Level 0

  Bare semiconductor (unpackaged).

- Level 1

  Packaged semiconductor or packaged electronic functional device. There are two cases to be distinguished regarding packaged integrated circuit (IC) devices. The first case entails a single semiconductor microcircuit within a suitable package. The second case entails several semiconductor microcircuits plus discrete chips on a suitable substrate. This entire package is generally referred to as a multichip module (MCM).

- Level 2

  Printed wiring assembly (PWA). This level involves joining the packaged electronic devices to a suitable substrate material. The substrate is most often an organic material such as epoxy-fiberglass board, or ceramic such as alumina. Level 2 is sometimes referred to as the circuit card assembly (CCA) or, more simply, the card assembly.

- Level 3

Electronic subassembly. This level refers to several printed wiring assemblies (PWAs), normally two, bonded to a suitable backing functioning both as a mechanical support frame and a thermal heat sink. Sometimes this backing, or support frame, is called a sub-chassis.

- Level 4

Electronic assembly. This level consists of a number of electronic subassemblies mounted in a suitable frame. An electronic assembly, then, is a mechanically and thermally complete system of electronic subassemblies.

- Level 5

System. This refers to the completed product.

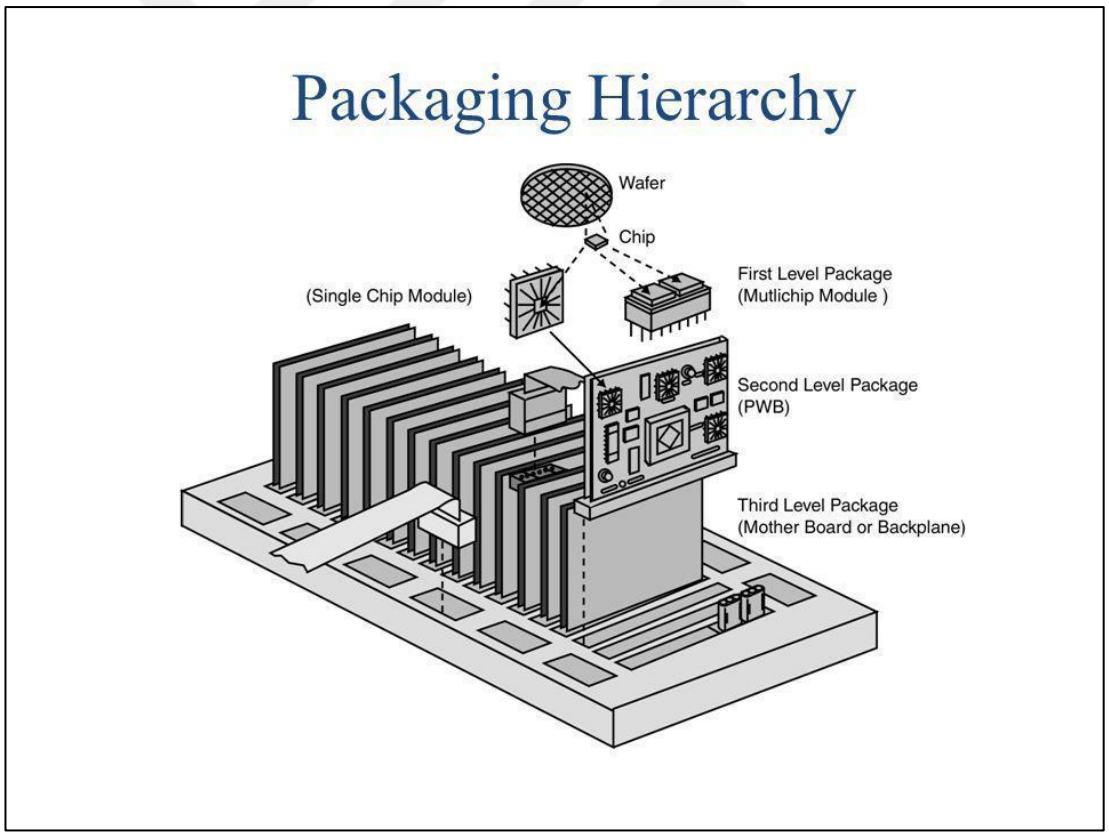

Figure 1.4: Electronic packaging hierarchy.

If heat is not taken at a rate equal to or higher than the production rate, components such as device temperatures will continue to increase, which can significantly reduce reliability and performance, as well as malfunction of the devices. These failures can cause huge problems especially in data centers, super speed computers, military vehicles (tanks, aircraft, robotics systems) and avionics systems. System - data security, loss of strategic space, large material and money losses and life safety are the result of failures in these components. Electronic cooling designs also differ according to the level of electronic packaging.

1.1. Cooling Techniques of Electronic Devices

Determining the optimum cooling technique at electronic packaging levels is very important for the safety of electronic components. The components used in electronic packaging levels to create the optimum design;

- Features,
- Heat power,
- Dimensions of designs according to chip or package levels
- Volume of designs according to chip or package levels
- Heat transfer coefficients of materials used
- Determining the working environment of the devices are very important.

When the developing technology and needs are considered, the features that should be considered in electronic cooling system designs should be as follows.

- Electronic cooling system should be selected for electronic devices.
- Keep devices within safe temperature range.
- Provide high heat dissipation.
- Cooling parts should fit to the desired dimensions and volumes.
- Material optimization should be done to reduce heat conduction resistance.
- Must be low cost.

- The safety of each step of the electronic packaging levels should be at the forefront.
- Comply with various standards.
- Must work in harsh climatic conditions.

Electronic cooling techniques are classified as follows in literature and commercial applications [10], [11].

- Radiation and free convection
- Forced air-cooling
- Forced liquid cooling
- Liquid evaporation.

The above categories of electronic cooling systems are classified as follows according to the use of coolant [12].

- Air cooling
- Liquid (evaporation) cooling
- Refrigeration cooling

- Air Cooling

Heat dissipation in this cooling technique is provided by air. These techniques are used as a cooling method for electronic components that require very low cooling. Air cooling is divided into two as natural convection and forced convection. In forced air cooling, the heat transfer coefficient is quite limited, although it is higher than natural convection. Generally, the air electronic cooling method is used for cooling CPUs, power transistors, power diodes. This method is low cost, simple and reliable.

The most common use known are heat sinks that provide natural and forced air with increased heat transfer surface area. Heat sinks used in different electronic packaging levels can be manufactured in different geometries and different types according to the heat load and design. Examples of different design for air cooling techniques are given in Figure 1.5.

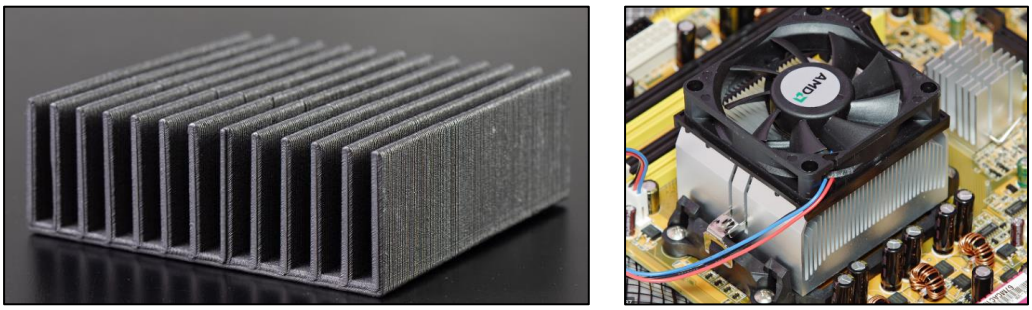

a) b)

Figure 1.5: a) Natural convection, b) Forced convection air cooling techniques.

- Liquid (Evaporation) Cooling

Various types of liquid cooling systems are used for electronic cooling. These include heat pipes, heat pump, microchannels, spray cooling, phase change material (PCM) based cooling, thermoelectric cooling.

Liquid electronic cooling systems are divided into passive and active systems. Passive cooling systems use capillary or gravitational buoyancy forces to circulate the working fluid. Active cooling systems use a pump or compressor for higher cooling capacity and improved performance.

Heat Pipes: The heat pipes that are passive cooling system, use for cooling electronic devices such as computer, laptop, telecommunication and satellite modules. To work based on the phase change of working fluid inside the pipes. Heat pipes occur of pipe, wick and cooling fluid. This pipe consists of three regions (evaporator, adiabatic and condensing region) [8]. The wick is the most important part. It is mostly mounted at the inner wall of the pipe. The wick supplies as capillary pumping. The fluid is driven by wick from the condenser section to the evaporator against the gravity. The working principle of a heat pipe is based on phase change heat transfer inside a pipe. The evaporator region is heated from an external heat source (like an electronic device or chip), the liquid is evaporated there. Thus, the fluid vapor pressure rises. Pressure difference occurs in the axial direction that pushes the vapor from the evaporator to the condenser. Vapor, condenses releasing the latent heat of vaporization to the heat sink and the turns back to liquid as Figure 1.6.

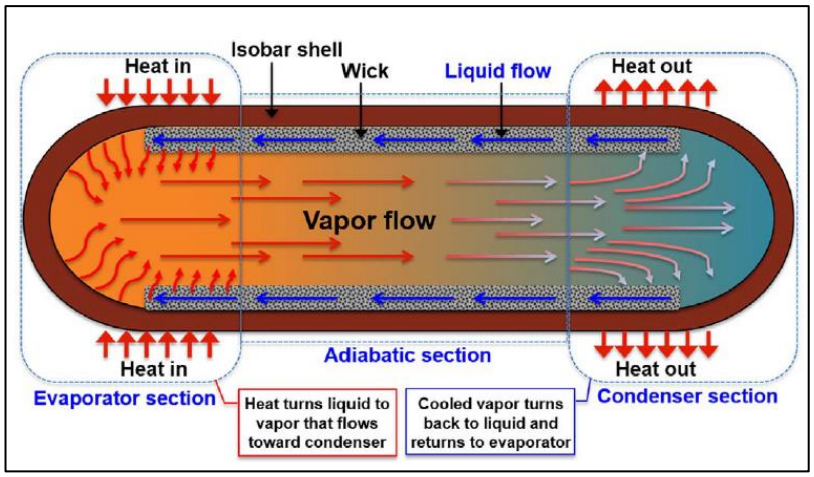

Figure 1.6: Working principle and schematic of a heat pipe.

a) b)

Figure 1.7: a) Pictures of heat pipe without fan, b) Picture of heat pipe with fan.

Heat Pumps; Heat pumps transfer heat from a low temperature fluid to another high temperature fluid. Heat pumps are used for medium cooling needs and are not applied to electronics cooling particularly high heat flux device.

Thermoelectric Cooling; Thermoelectric cooler (TEC) produces heat flux between the junctions of two different types of semiconductors through the Peltier effect. Semiconductors transfers heat from one side of the device to the other with consumption of electrical energy. The main component of a TEC is a series of two different conductors as P and N type semiconductors [8]. The working principle of a heat pipe is based on electrical current on semiconductors. Firstly, voltage is applied to the free ends of the two different conducting elements resulting in current flow through the P and N semiconductors.

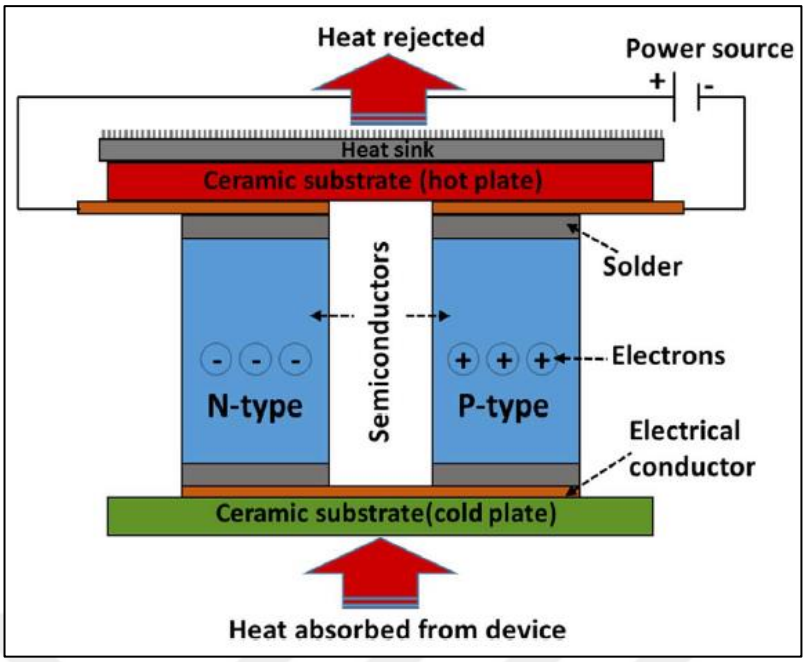

Figure 1.8: Working principle and schematic of thermoelectric cooling.

Coolants for Liquid Cooling; There are many traditional coolants, which are used in various electronics liquid cooling systems. It is important to select the best coolant for cooling system. There are some general requirements for coolant. Coolant which are chosen depend on the type of cooling systems and electronic devices. Coolants are used for electronics should be inexpensive, flammable, non-toxic and have excellent thermophysical properties. Their features must include high thermal conductivity, specific heat and heat transfer coefficient as well as low viscosity. Coolants must be compatible with the materials of the cooling system components as well as the devices. The chemical compatibility of the coolant with chip and other electronic packaging materials should be considered (non-corrosive).

- Vapor Compression Cooling

When forced air and liquid cooling systems are insufficient in electronic devices that produce very high heat and in the electronic package level, a vapor compression refrigeration cycle is used instead of the other cooling techniques. In order to ensure the safety of electronic devices and to reach below critical temperatures, vapor compression refrigeration cycles are used in military systems, radar systems, avionics systems, aircraft, super-speed computers and data centers, especially in difficult climatic conditions.

The vapor compression refrigeration cycle can be shown as the reverse Rankine cycle. In this cycle, heating or cooling is provided by utilizing the phase change of a refrigerant. The latent heat of vaporization of the refrigerant is used to transfer large amounts of heat energy, and changes in pressure are used to control when the refrigerant expels or absorbs heat energy.

CFC, HCFC, CO2 and ammonia fluids are generally used in refrigeration cycles. Due to the high ozone depletion potential (ODP) and global warming potential (GWP) according to European Union directives, the use of CFC and HCFC refrigerants is gradually reduced. The use of high CO_2 emission refrigerants starting in 2011 is aimed to be reduced by 78% until 2050. However, some sectors and applications are excluded in line with this directive. The reasons for exclusion in these sectors; safety, certifications and fluid properties [13]. The most preferred fluid in special area that military equipments and special applications is R134A because of its high critical temperature (101,1 ^{o}C). Vapor compression system occurs four main device that are given at Figure 1.9.a) [14].

- Compressor: The vapor refrigerant is compressed and provides the necessary mechanical energy to the system.
- Condenser: Absorbs heat (at constant pressure) from the working environment and transfers it to a high temperature source.
- Throttling valve: It reduces the refrigerant to constant enthalpy evaporator working pressure.
- Evaporator: The evaporation of the working medium while it absorbs heat from the low temperature reservoir.

In Figure 1.9.b) the P-h graph of the vapor compression cycle for cooling operations is as follows [14].

- 1-2 isentropic compression
- 2-3 constant pressure heat rejection in the condenser
- 3-4 throttling in an expansion valve
- 4-1 constant pressure heat addition in the evaporator

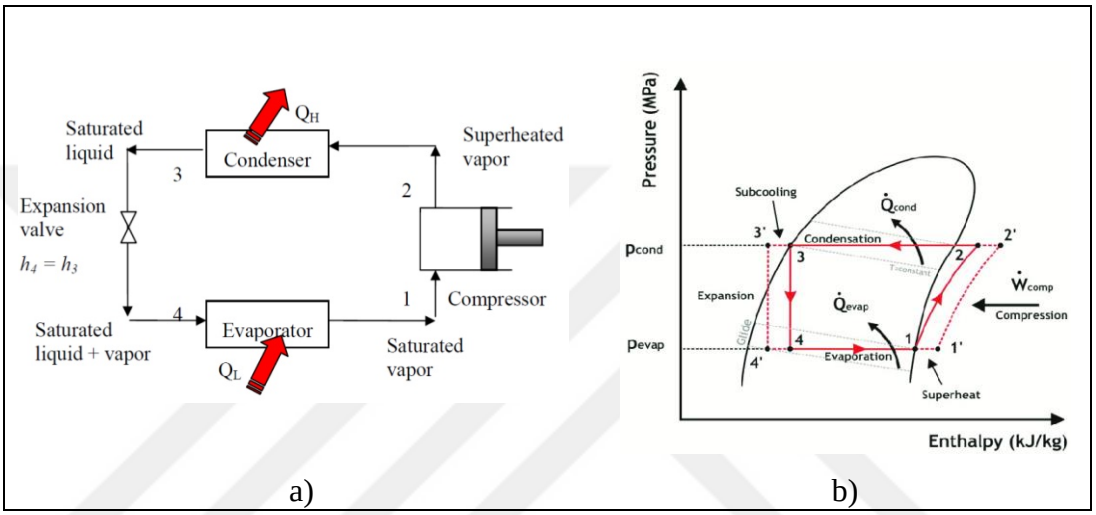

Figure 1.9: a) Vapor compression refrigeration cycle, b) P-h graph.

In the case of vapor compression systems used in electronic cooling, the following specifications must be considered.

- CMOS chip/CPU performance
- Cost of refrigeration system
- Life cycle cost
- Volume, mass
- Power consumption
- Reliability of refrigeration/packaging
- Vibration

2. THE LITERATURE REVIEW

Over the past forty years, there have been many studies in the literature examining the heat transfer of different refrigerants in different pipe diameters. One of the two most important factors triggering that is the need for high heat dissipation with evolving electronic technology and the other is the Montreal Protocol [15]. Due to the limitations in these area (such as settlement difficulties, high heat load per unit area, fluid regulation, etc.), researchers have been directed towards the improvement of heat transfer in mini-micro channels and alternative refrigerants. As a result, intensive analytical and experimental studies have been carried out for the boiling and condensation of in-pipe flow and the heat transfer coefficient correlations have been used in the design of mini-channel heat exchangers [16]-[19]. In vapor compression refrigeration (VCR) systems customized for electronic cooling, the evaporator is usually customized. The condenser can be used as finned-tubes and minichannel type according to the layout and dimensions of the system. Evaporator designs are as important as condenser designs. The evaporator is especially customized for heat load, application, dimensions of the electronic system and space requirements. In addition, the critical operating conditions of the electronic part in which the system is installed are the biggest factors.

Customized vapor compression refrigeration systems designs have been investigated experimentally and analytically in electronic systems due to high heat loads and operating conditions.

Recently, miniature vapor compression refrigeration systems have been used in the literature in different designs for electronic systems. In a study, it was aimed to keep the surface temperature under critical temperature by using a mini-channel evaporator for cooling the low level electronic package. A microchannel evaporator that length of 20 mm was used heating power of 100 W, 150 W and 200 W with an adjustable speed compressor. The performance efficiency of this specially designed cooling system has been evaluated with different superheat and thermal loads. The results have shown that the compressor speed and heat load effect the system COP and surface temperature [20].

Wiriyasart at al. for a dual processor super speed workstation computer, the heat sink and thermoelectric air cooling system used for CPU cooling were investigated experimentally between 0-100%. The authors measured cpu surface temperatures at certain points and were determined the air flow direction of the fan used for the test. Although the temperature of the CPUs improved in the thermoelectric cooling system, energy consumption increased [21].

In another study, an evaporator was designed for chip cooling of a computer for R600A fluid at different flow rates by using a evaporator/heat pipe hybrid system. Heat transfer coefficients and surface temperatures at 30 - 60 W heat load were investigated experimentally. Hybrid system was occurred heat pipe and small scale refrigerant cycle. Condensing region of heat pipe was connected designed evaporator of refrigerant system. Copper tubes for heat transfer parameters, such as thermal resistances and frictional factors, were calculated. This values compared test results and heat transfer coefficients were calculated with different heat load and mass flow rate. The main results that comparison evaporator model and experimental results was shown on evaporator heat transfer coefficient. This study has given results successful calculated model [22].

Another customized electronic cooling system is the cold plate designs. In the vapor compression refrigeration cycle, a flat surface is formed with a material such as copper or aluminum. System cools the copper or aluminum plate. The cooled plate is combined with electronic circuits. Thus, cooling of the electronic circuits is provided. Cold plates, which are customized according to electronic package levels, are the most preferred method of vapor compression cooling systems.

Mancin at al. the experimental analysis of a mini vapor cycle system for electronic in avionic applications. The authors aim kept below 70 ^{o}C wall temperature with cold plate. Cold plate was made from copper with dimension 400 mm long 20 mm wide and 10 mm thickness. The tests were performed with R134A and 37-374 W heat load at different evaporation (5 ^{o}C, 15 ^{o}C, 25 ^{o}C) and condensation temperatures (30 ^{o}C, 40 ^{o}C, 50 ^{o}C, 60 ^{o}C). According to the measurement results, the temperature distributions of the cold plate are emphasized the presence of three different regions as two phase heat transfer region a dryout region and a post dryout region [23]. In another study, the cold plate design was used for CPU cooling of 25 x 25 mm. Evaporator designs and COP calculations were made at 100 - 200 W heat load, different fluid flow rates and different compressor speed.

Evaporator design was made with minichannel. Kandlikar correlation was used from the literature for thermal design. High COP was detected to be at high heat load at medium compressor speed. In addition, the system was reported to remain below the CPU critical temperature of 60 ^{o}C under this operating condition [24].

In another study, electronic cooling study included a evaporator cooling capacity of 400 W at 25 ^{o}C. Heat loads were had varied range between 210 to 400 W. The author was used a adjustable compresor speed with PID control. The models results were compared with experiment data. The model of evaporator with maximum error of 10 % at 400 W of evaporator heat load and with an average error of 5 % for all loads [25].

Zilio at al. a compact heat pipe and air-cooled vapor compression system were used in a hybrid system for avionic cooling. In this study, it was aimed to use the avionic system under critical temperatures by using a customized minichannel heat exchanger [26].

Li and Mudawar gave the datas of incorporating two phase microchannel heat sink as an evaporator in a VCR system. The authors were used new correlations for pressure drop and two-phase heat transfer coefficient for thermal design. The microchannel heat sink that authors were used occured of a polycarbonate cover plate, fiberglass housing, a microchannel oxygen-free copper heat sink and support plate. They were reported to effect of evaporator geometry, as hydraulic diameter and channel aspect ratio. They were observed the changing temperature along the evaporator channel at different flow rates and compared them with their calculations. Especially at 200W heat load, evaporation temperature and wall temperature changes and heat transfer coefficients at different flow rates were compared. they were reported that the system reduces the temperature of the electronic circuit wall surface from 70 ^{o}C to 40 ^{o}C at a constant flow rate and 500 W heat load. [27].

In an another experimental study was worked with a minichannel evaporator to remove 400 W heat load. The minichannel evaporator has 41 rectangular channels (0.8 mm x 2.3 mm) which made by aluminum. evaporator was used as a cold layer to realize heat dissipation. In the system where 100 g R134A was charged, a hand-operated needle valve was used as the expansion valve. The authors evaluated system performance at different air temperatures for condenser. The experimental results showed that the system dissipated CPU heat fluxes of 40-75 W/cm^2 and keep the device temperature below 85 ^{o}C [28].

2.1. Aim of the Study

It is very important that electronic circuits and boards of high-speed computers, military vehicles, etc. systems remain below the critical operating temperatures. If these critical temperatures are exceeded, electronic circuits will become inoperable. As a result, it seriously damages critical data loss and system security. Electronic circuits should not reach critical operating temperature, especially in order to prevent adverse conditions in military systems.

In this study, a vapor compression refrigeration system for computers which need to high cooling applications have been studied for maintain the uniform chip surface temperature below the study aim at 85 ^{o}C. At the same time a calculation module, for evaporator optimization and design, has been developed. The minichannel evaporator designs were calculated by selecting from heat transfer and pressure drop equations in literature. The evaporator, designed and produced in the test section, was equipped with 200 mm x 200 mm silicon heaters that model electronic chips according to different heat loads (100 – 500 W), and the aluminum layer, 2 mm, was sequentially joined. Chip surface temperatures were measured according to constant evaporation temperature and variable heat load and the results were compared with the generated calculation module.

3. CALCULATION METHOD and THERMAL DESIGN

Minichannel evaporator designs can be calculated according to the required cooling capacity and requirement size. The thermal design can also be formed according to the use of the evaporator. At this point, optimization of different geometries is possible. In this thesis, the calculation module is based on the scenario of insulating one surface of the evaporator and cooling the electronic circuits together with the silicon heater.

The evaporator calculation module is created in MATHCAD PRIME 4.0 (2939163-PKG-7502-L). In the calculation module, the surface area of the heat exchanger is divided into a certain number (step by step) according to the desired cooling load and individual calculations are made for each area. Each surface area can be defined as 'number of segments' in the calculation module as user-defined.

The area between each entry-exit point is the thermal calculation zone. In divided areas, the calculations are taken sequentially as a series. The resulting value of one field is taken as the input value of the next field. Figure 3.1 schematically shows the division of the evaporator into the calculation zones according to the dividing points for the step-by-step calculation (SBS).

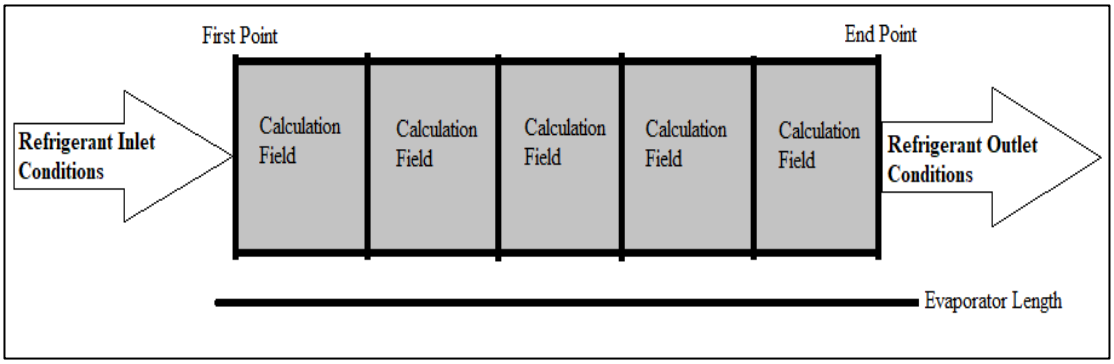

Figure 3.1: SBS calculation area.

The output data of each calculation area is considered as input data for the other sub-area and the calculation is performed iteratively and serially. Dimensionless numbers and physical properties are calculated separately for each point.

In the calculation area, at the inlet and outlet temperatures for the assigned refrigerant; Heat transfer coefficient, viscosity, specific heat, Prandtl number and density values are printed on the program. Nusselt numbers and total heat transfer coefficient are calculated according to thermo-physical properties.

3.1. Calculation Algorithm Steps

The Calculation module was made in Mathcad algorithm that explained below step by step.

- Heat load (evaporator cooling capacity), operating conditions (refrigerant inlet-outlet temperature, superheat, condensation temperature, subcooling), evaporator geometric parameters (Length, number of pipes, diameter, pipe thickness, etc.) are assigned as input values to the calculation module.
- Refrigerant fluid selection is made.
- The heat transfer area is calculated for the given geometry. The calculation zones are divided by the specified number along the length of the evaporator.
- For calculation areas, the thermo-physical properties of refrigerant are calculated at the input - output temperatures.
- The refrigerant mass flow rate is calculated according to the given heat load by the Formula 3.1.

$$\dot{m} = \frac{q''}{(h_o - h_i)} \tag{3.1}$$

- The fluid pressure loss is calculated for the single phase (vapor region) and two phase (evaporation region) that occur in the evaporator.
- Nusselt number, heat transfer coefficient, surface temperatures along the length of the evaporator are calculated.

- Calculation algorithm flow chart is given in Figure 3.2., and the interface of evaporator calculation module is given in Table 3.1.

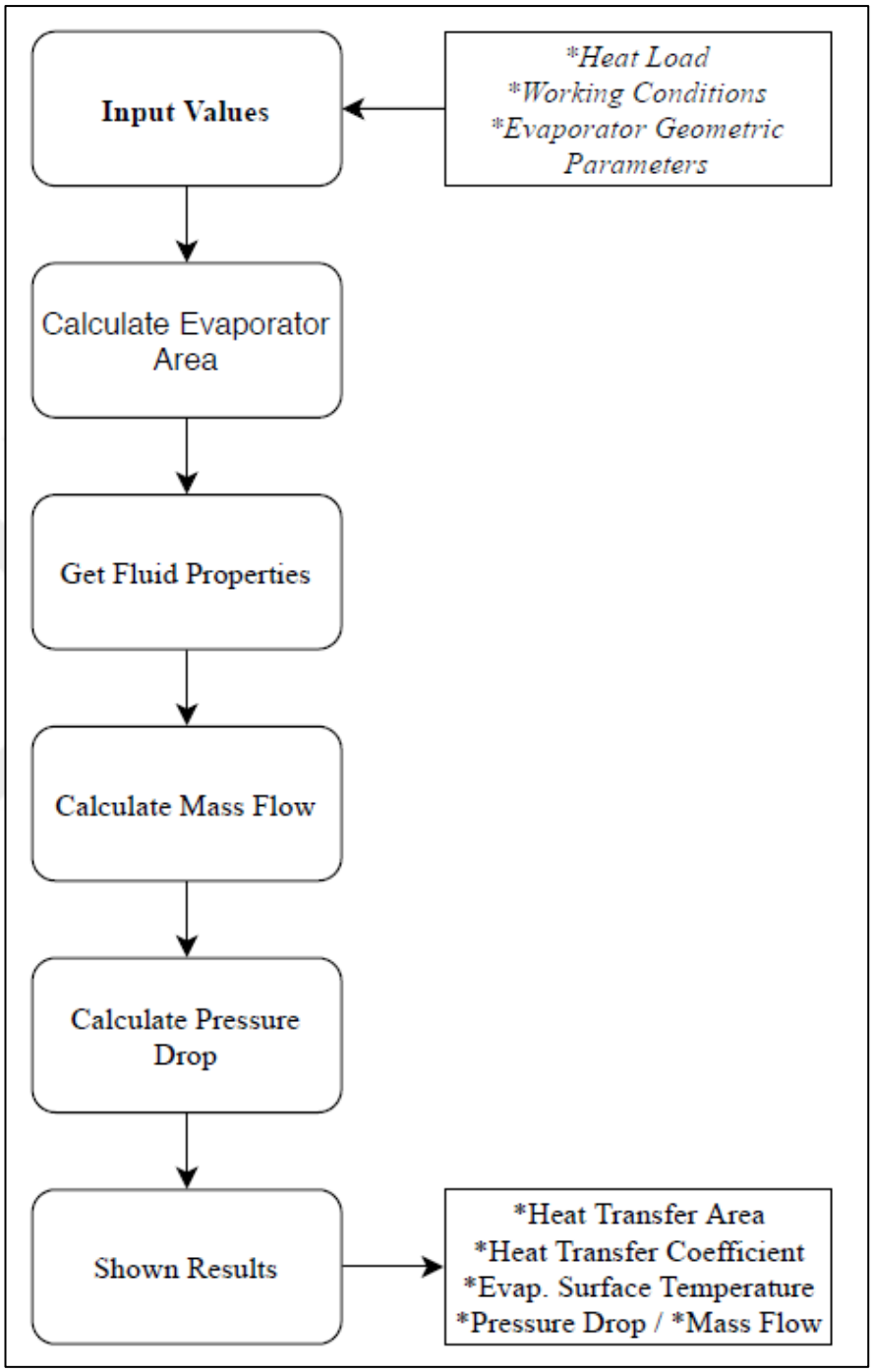

Figure 3.2: Calculation algorithm flow chart.

Table 3.1: Calculation module interface.

Working Conditions	**Sample Value**	**Unit**
Heat Power	500	W
Evaporator Temperature	5	^{o}C
Superheat	1	K
Condenser Temperature	40	^{o}C
Subcooling	1	K
Type of Refrigerant	R134A	
Evaporator Geometry	**Parameter**	**Unit**
Evaporator Length	200	mm
Number of Tubes	5	
Number of Segments	20	
Tube Major Diameter (D_{maj})	22	mm
Tube Minor Diameter (D_{min})	3	mm
Tube Wall Thickness (t_{tube})	0,32	mm
Channel Width (C_w)	3	mm
Number of Channels in Tube (NC)	12	

3.2. Evaporator Design

The minichannel evaporator, which pipes are designed by placing the horizontally, is designed in different geometries. The geometric parameters affecting the performance of the minichannel evaporator are as follows.

- Number of channels in a pipe
- Number of pipes
- Pipe wall thickness
- Total number of pipes at the evaporator
- Evaporator length

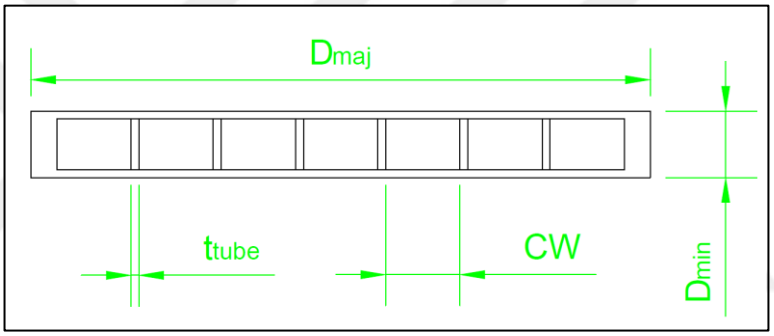

Figure 3.3: Cross-sectional view of a sample pipe.

The heat transfer surface area of a minichannel evaporator is calculated according to the following equations. Inner flow area, outer surface area, total flow area and hydraulic diameter are calculated.

$$NCT = N_{tube}NC \tag{3.2}$$

$$C_H = D_{min} - 2t_{tube} \tag{3.3}$$

$$C_W = \frac{D_{maj} - (NC + 1)t_{tube}}{NC} \tag{3.4}$$

$$D_h = \frac{4C_H C_W}{2(C_H + C_W)} \tag{3.5}$$

$$D_h = D_{in} \tag{3.6}$$

$$\beta = \frac{C_H}{C_W} \tag{3.7}$$

$$A_{tubebare} = N_{tube}\, 2\left[\left(E_L\, D_{maj}\right) + \left(E_L\, D_{min}\right)\right] \tag{3.8}$$

$$A_{inside} = N_{tube}\left(2C_H + C_W\right) NC\, E_L \tag{3.9}$$

$$A_{tubecrossreal} = C_H\, C_W\, NCT \tag{3.10}$$

$$A_{tubeDh} = \frac{\pi\, {D_h}^2}{4} NCT \tag{3.11}$$

- Fluid Properties

For the thermophysical properties of refrigerant, the Mathcad PRIME 4.0 program for Water (H_2O), CO_2, R134A, Nitrogen, Argon, Ammonia, R449A, R404A, R410A, propane and other fluids uses the CoolProp.dll (NIST REFPROP) plug-in.

CoolProp.dll R134A fluid properties are printed using the codes defined in CoolPropFluidProperties.xmcd according to the desired thermos-physical value, temperature, pressure or dryness with the following equations. The enthalpy of the fluid, heat conduction coefficient, viscosity, specific heat, Prandtl number and density are the thermo-physical properties required for calculation. The definitions giving the saturated liquid - vapor thermophysical values are as follows.

$$h_v = \text{FluidProp}(\text{"H"}, \text{"T"}, Tevap, \text{"Q"}, 1, \text{"R134A"}) \tag{3.12}$$

$$h_l = \text{FluidProp}(\text{"H"}, \text{"T"}, Tevap, \text{"Q"}, 0, \text{"R134A"}) \tag{3.13}$$

$$c_{pv} = \text{FluidProp}(\text{"C"}, \text{"T"}, Tevap, \text{"Q"}, 1, \text{"R134A"}) \tag{3.14}$$

$$c_{pl} = \text{FluidProp}(\text{"C"}, \text{"T"}, Tevap, \text{"Q"}, 0, \text{"R134A"}) \tag{3.15}$$

$$\mu_v = \text{FluidProp}(\text{"V"}, \text{"T"}, Tevap, \text{"Q"}, 1, \text{"R134A"}) \tag{3.16}$$

$$\mu_l = \text{FluidProp}(\text{"V"}, \text{"T"}, Tevap, \text{"Q"}, 0, \text{"R134A"}) \tag{3.17}$$

$$\rho_v = \text{FluidProp}(\text{"D"}, \text{"T"}, Tevap, \text{"Q"}, 1, \text{"R134A"}) \tag{3.18}$$

$$\rho_l = \text{FluidProp}(\text{"D"}, \text{"T"}, Tevap, \text{"Q"}, 0, \text{"R134A"}) \tag{3.19}$$

$$k_v = \text{FluidProp}(\text{"L"}, \text{"T"}, Tevap, \text{"Q"}, 1, \text{"R134A"}) \tag{3.20}$$

$$k_l = \text{FluidProp}(\text{"L"}, \text{"T"}, Tevap, \text{"Q"}, 0, \text{"R134A"}) \tag{3.21}$$

$$Pr_v = \frac{\mu_v \, c_{pv}}{k_v} \tag{3.22}$$

$$Pr_l = \frac{\mu_l \, c_{pl}}{k_l} \tag{3.23}$$

The definitions that give the thermo-physical values of the fluid at a certain temperature and pressure are as follows.

$$h(T,P) = \text{FluidProp}(\text{"H"}, \text{"T"}, T, \text{"P"}, P, \text{"R134A"}) \tag{3.24}$$

$$c_p(T,P) = \text{FluidProp}(\text{"C"}, \text{"T"}, T, \text{"P"}, P, \text{"R134A"}) \tag{3.25}$$

$$\mu(T,P) = \text{FluidProp}(\text{"V"}, \text{"T"}, T, \text{"P"}, P, \text{"R134A"}) \tag{3.26}$$

$$\rho(T,P) = \text{FluidProp}(\text{"D"}, \text{"T"}, T, \text{"P"}, P, \text{"R134A"}) \tag{3.27}$$

$$k(T,P) = \text{FluidProp}(\text{"L"}, \text{"T"}, T, \text{"P"}, P, \text{"R134A"}) \tag{3.28}$$

$$Pr(T,P) = \frac{\mu(T,P) \, c_p(T,P)}{k(T,P)} \tag{3.29}$$

The definitions that give the thermophysical values of the fluid at a certain temperature and dryness are as follows.

$$h(T,x) = \text{FluidProp}(\text{"H"}, \text{"T"}, T, \text{"Q"}, x, \text{"R134A"}) \tag{3.30}$$

$$c_p(T,x) = \text{FluidProp}(\text{"C"}, \text{"T"}, T, \text{"Q"}, x, \text{"R134A"}) \tag{3.31}$$

$$\mu(T,x) = \text{FluidProp}(\text{"V"}, \text{"T"}, T, \text{"Q"}, x, \text{"R134A"}) \tag{3.32}$$

$$\rho(T,x) = \text{FluidProp}(\text{"D"}, \text{"T"}, T, \text{"Q"}, x, \text{"R134A"}) \tag{3.33}$$

$$k(T,x) = \text{FluidProp}(\text{"L"}, \text{"T"}, T, \text{"Q"}, x, \text{"R134A"}) \tag{3.34}$$

$$Pr(T,x) = \frac{\mu(T,x) \, c_p(T,x)}{k(T,x)} \tag{3.35}$$

- Thermal Design

The minichannel evaporator designs were calculated by selecting from heat transfer and pressure drop equations in literature [19]. Nusselt number was defined for three different flow characteristics in single phase flow. The refrigerant is often in the turbulence model in minichannel pipes.

$$\dot{G} = \left[\frac{4\,\dot{m}}{\pi\, D_{in}^2\, NC}\right] \tag{3.36}$$

$$V = \frac{\dot{G}}{\rho} \tag{3.37}$$

$$Re_g = \left[\frac{\dot{G}\, D_{in}}{\mu}\right] \tag{3.38}$$

$$Pr = \frac{\mu\, c_p}{k} \tag{3.39}$$

$$Nu = \begin{cases} Nu_{Laminar}, & Re_g \leq 2500 \\ Nu_{Tur}, & Re_g > 4000 \\ Nu_{TR}, & 2500 < Re_g \leq 4000 \end{cases} \tag{3.40}$$

The general definition of Nusselt number in the laminar region is given in Equation 3.44.

$$Nu_{L1} = 3.66 \tag{3.41}$$

$$Nu_{L2} = 1.615 \text{ x} \left(Pr\, Re_g \frac{D_{in}}{L_{tube}}\right)^{\frac{1}{3}} \tag{3.42}$$

$$Nu_{L3} = \left(\frac{2}{1 + 22 \text{ x } Pr}\right)^{\frac{1}{6}} \left(Re_g\, Pr \frac{D_{in}}{E_L}\right)^{\frac{1}{2}} \tag{3.43}$$

$$Nu_{Laminar} = [Nu_{L1}^3 + 0.7^3 + (Nu_{L2} - 0.7)^3 + Nu_{L3}^3]^{\frac{1}{3}} \tag{3.44}$$

The general definition of Nusselt number in the transition zone is given in Equation 3.46.

$$\gamma = \frac{\mathrm{Re_g} - 2300}{4000 - 2300} \tag{3.45}$$

$$\mathrm{Nu_{TR}} = \left((1-\gamma)\ \mathrm{x}\ \mathrm{Nu_{Laminar}}\right) + \left(\gamma\ \mathrm{x}\ \mathrm{Nu_{Tur}}\right) \tag{3.46}$$

In the calculation of the heat transfer coefficient in the turbulence region, Churchill expression was used for the coefficient of friction and Gnielinski expression was used for the Nusselt number (Equation 3.49) [18], [29].

$$\zeta = 8\left[\left(\frac{8}{\mathrm{Re_g}}\right)^{12} + \left(\frac{1}{(\alpha\alpha + \beta\beta)^{1.5}}\right)\right]^{\frac{1}{12}} \tag{3.47}$$

$$\alpha\alpha = 2.457 \ln\left[\frac{1}{\left(\frac{7}{\mathrm{Re_g}}\right)^{0.9} + \left(\frac{0.27\mathrm{k_s}}{\mathrm{D_{in}}}\right)}\right]^{16} \tag{3.48}$$

$$\beta\beta = \left(\frac{37500}{\mathrm{Re_g}}\right)^{16} \tag{3.49}$$

$$\mathrm{Nu_{Tur}} = \frac{\left(\frac{\zeta}{8}\right)\left(\mathrm{Re_g} - 1000\right)\mathrm{Pr}}{1.07 + 12.7\left(\frac{\zeta}{8}\right)^{\frac{1}{2}}\left(\mathrm{Pr}^{\frac{2}{3}} - 1\right)}\left[1 + \left(\frac{\mathrm{D_{in}}}{\mathrm{E_L}}\right)^{\frac{2}{3}}\right] \tag{3.50}$$

$$\mathrm{h_{HTC,SP}} = \mathrm{Nu}\frac{\mathrm{k}}{\mathrm{D_{in}}} \tag{3.51}$$

The two phase correlation is used from Shah R. K and Shah M. M.'s Equations [16], [30], [31]. The correlation consists of fluid surface parameters. The heat transfer equations for a correction coefficient contains Boiling, Froude and Convection Numbers. The general definition of heat transfer coefficient in the turbulence zone is given in Equation 3.67.

$$\dot{G} = \left[\frac{4\,\dot{m}}{\pi\, D_{in}^2\, NC}\right] \tag{3.52}$$

$$Pr_v = \frac{\mu_v\, c_{pv}}{k_v} \tag{3.53}$$

$$Pr_l = \frac{\mu_l\, c_{pl}}{k_l} \tag{3.54}$$

$$V = \left[\frac{\dot{G}}{\rho_l}\right] \tag{3.55}$$

$$Re = \left[\frac{G\, D_{in}\ (1-x)}{\mu_l}\right] \tag{3.56}$$

$$Bo = \frac{q''}{\dot{G}\,(h_v - h_l)} \tag{3.57}$$

$$Fr = \frac{\dot{G}^2}{\rho_l^2\, g\, D_{in}} \tag{3.58}$$

$$Co = \left[\left(\frac{1}{x} - 1\right)^{0.8}\ \left(\frac{\rho_v}{\rho_l}\right)^{0.5}\right] \tag{3.59}$$

$$N = \begin{cases} 0.38\ x\ Co\ x\ Fr^{-0.3}, & Fr \le 0.04 \\ Co, & Fr > 0.04 \end{cases} \tag{3.60}$$

$$h_{CC,1} = 1.8N^{-0.8} \tag{3.61}$$

$$h_{CC,2} = \begin{cases} 230\sqrt{Bo}, & Bo \ge 3\ 10^{-5} \\ 1 + 46\sqrt{Bo}, & Bo < 3\ 10^{-5} \end{cases} \tag{3.62}$$

$$h_{CC,3} = \begin{cases} 14.70\sqrt{Bo}e^{2.74N^{-0.1}}, & Bo \ge 1.1\ 10^{-5} \\ 15.43\sqrt{Bo}e^{2.74N^{-0.1}}, & Bo < 1.1\ 10^{-5} \end{cases} \tag{3.63}$$

$$h_{CC,4} = \begin{cases} 14.70\sqrt{Bo}e^{2.74N^{-0.15}}, & Bo \ge 1.1\ 10^{-5} \\ 15.43\sqrt{Bo}e^{2.74N^{-0.15}}, & Bo < 1.1\ 10^{-5} \end{cases} \tag{3.64}$$

$$h_{CC} = \begin{cases} \max(h_{CC,1}, h_{CC,4}), & N \le 0.1 \\ \max(h_{CC,1}, h_{CC,3}), & 0.1 < N < 1 \\ \max\left(h_{CC,1}, h_{CC,2}\right), & N > 1 \end{cases} \tag{3.65}$$

$$h_{HTC,SP,Liquid} = \frac{k_l}{D_{in}} 0.023 Re^{0.8} Pr_l^{0.4} \tag{3.66}$$

$$h_{HTC,TP} = h_{CC} h_{HTC,SP,Liquid} \tag{3.67}$$

Pressure loss in single phase flow is given in equation 3.68 [17].

$$\Delta P = \zeta \frac{1}{2} \frac{L_{tube}}{D_{in}} \rho V^2 \tag{3.68}$$

Pressure loss in two phase correlation is used from Muller-Steinhagen equations [32].

$$A = \phi_l \frac{\dot{m}}{2\,\rho_l D_{in}} \tag{3.69}$$

$$B = \phi_g \frac{\dot{m}}{2\rho_g D_{in}} \tag{3.70}$$

$$\phi_l, \phi_g = \begin{cases} \phi_l = \dfrac{64}{Re_l}, \phi_g = \dfrac{64}{Re_g}, & Re_l, Re_g \leq 1187 \\ \phi_l = \dfrac{0.3164}{Re_l^{\frac{1}{4}}}, \phi_g = \dfrac{0.3164}{Re_g^{\frac{1}{4}}}, & Re_l, Re_g > 1187 \end{cases} \tag{3.71}$$

$$\Upsilon = A + 2(B - A)x \tag{3.72}$$

$$\Delta P_{TP} = \Upsilon(1 - x)^{\frac{1}{3}} + (Bx^3) \tag{3.73}$$

4. EXPERIMENTAL SETUP

An experimental setup for verification of the evaporator design software has been established. In this refrigerant system, a test section that has an electronic chips emitting heat were modeled. Electronic chips that produces heat in the range of 100-200 - 300 - 400 - 500 W have been modeled and the designed evaporator has been tested. The results were compared with the calculation module outputs.

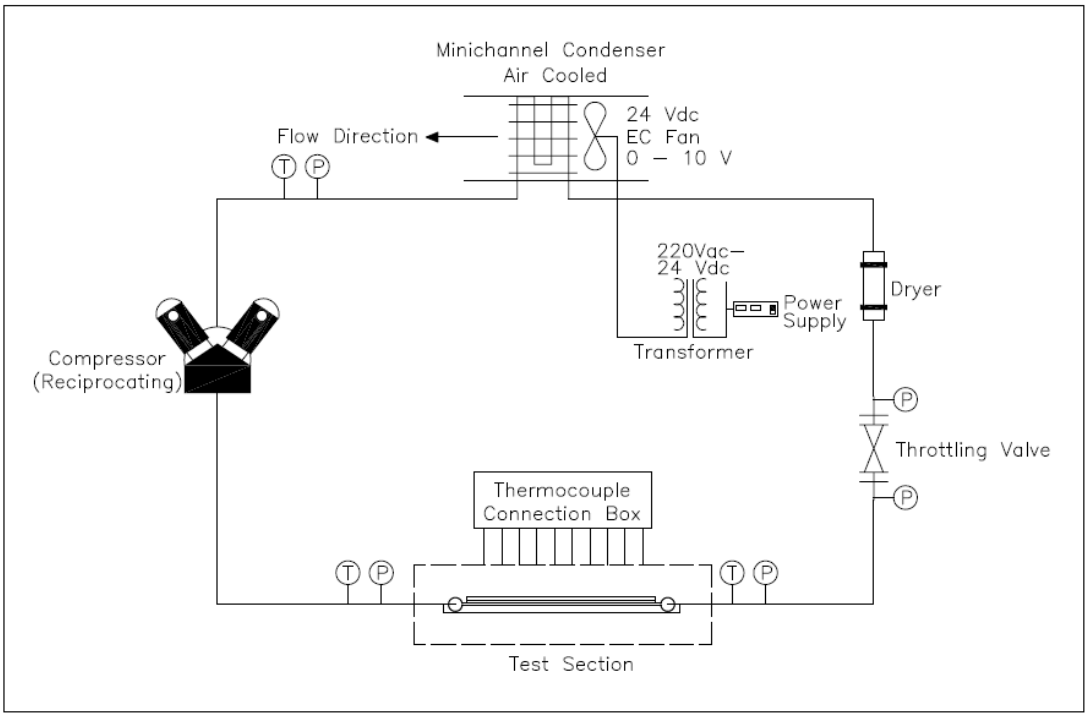

Figure 4.1: Schematic of experimental apparatus.

In Figure 4.1, the refrigeration system has four main components that are a compressor, a condenser, a throttling device and an evaporator which has without fins. Compressor is a hermetic reciprocating type, Embraco EM T6144Z, has maximum cooling capacity 671 W. In table 4.1, is shown compressor technical specifications. This compressor supplies different capacity at different working conditions for design parameters.

Table 4.1: Compressor technical data.

Brand / Model	Embraco EM T6144Z
Type	Hermetic reciprocating type
Refrigerant	R134A
Evaporation Temperature Range	-15 ^{o}C to 10 ^{o}C
Nominal Voltage/Frequency	220-240 V 50 Hz 1 ~ (Single phase)
Operating voltage range at 50 Hz	198 to 255 V

Evaporators designed for testing consist of a total of 48 minichannels with four pipes and 60 minichannels with five pipes. The pipes were horizontally soldered to the collectors. Pipes are 210 mm length, 25 mm wide, 3 mm high and 0.32 mm pipe wall thickness. Pipes were brazed in 15 mm diameter aluminum header. 3D view of evaporator 1 and 2 are given in Figure 4.2 and Figure 4.3.

Table 4.2: Evaporator specifications.

Specifications	**Evaporator 1**	**Evaporator 2**
Pipe Length	210 mm	210
Number of Pipe	5	4
Pipe Major Diameter	22 mm	22 mm
Pipe Minor Diameter	3 mm	3 mm
Pipe Wall Thickness	0.35 mm	0.35 mm
Pipe Channel Width	1.8 mm	1.8 mm
Number of Channel in Pipe	12	12
Total Circuit	60	48

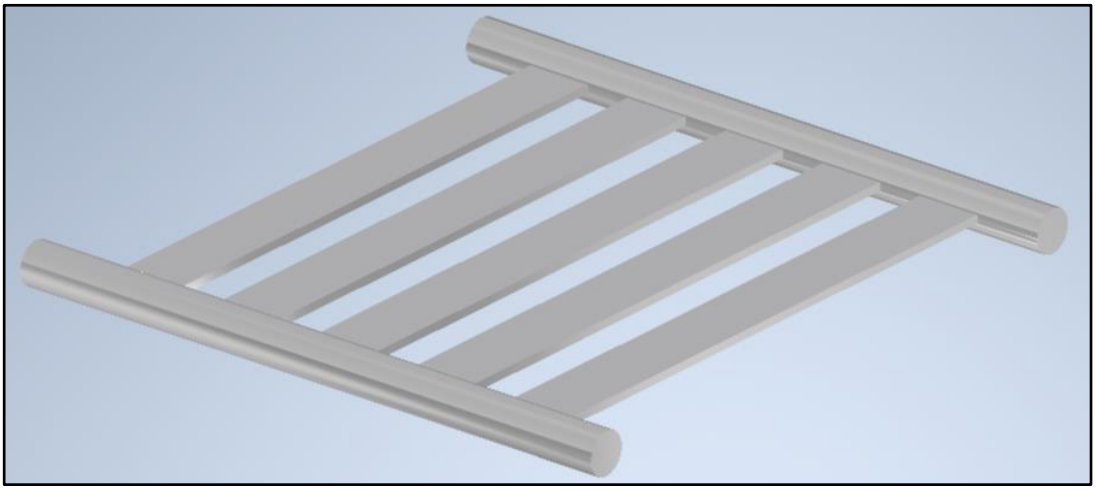

Figure 4.2: 3D view of evaporator 1.

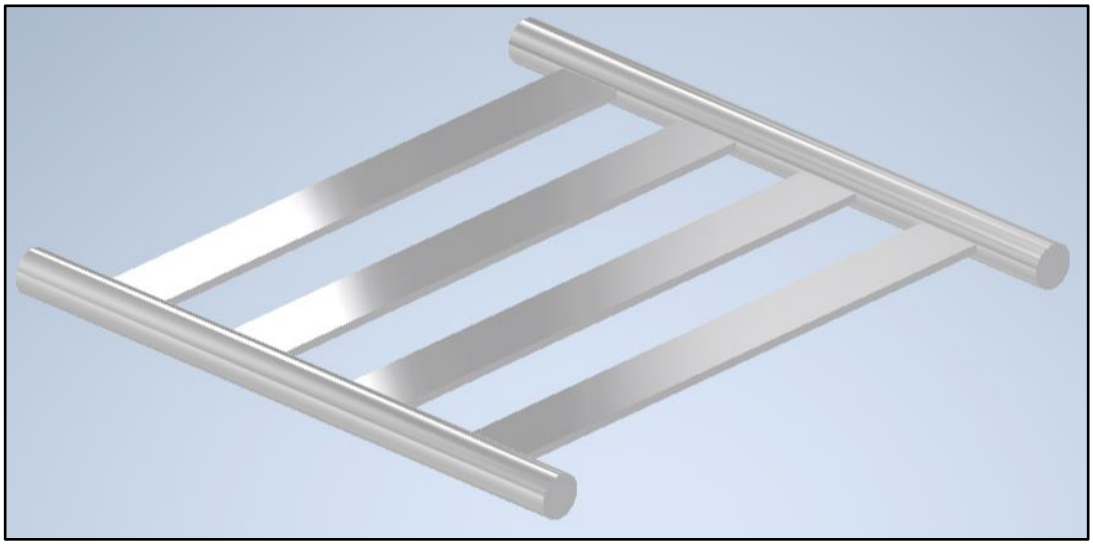

Figure 4.3: 3D view of evaporator 2.

The condenser used in the refrigerant system was specially designed and dimensioned for this work. The design of the condenser, like the evaporator design, was made with the calculated module. Condenser capacity control was done by a fan with EC motor. Technical specifications of condenser and fan are given in Table 4.3 and Table 4.4.

Table 4.3: Condenser specifications.

Microchannel Tube/Manifold	16 mm / 7 Ports / 20 mm Header
Fin Type	Louver 16 mm / 2.1 mm Pitch
Microchannel Height	198 mm
Microchannel Length	200 mm
Number of Fins	20
Number of Tubes	19
Pass Arrangement	3 Pass (11/5/3)

Table 4.4: Condenser fan specifications.

Type	EBM W1G200-HH77-52
Motor	M1G074-BF
Nominal Voltage	24 VDC
Speed	2950 rpm
Power Input	55 W
Current Draw	2.6 A

a) b)

Figure 4.4: a) Minichannel conderser, b) Condenser EC fan.

Since the electronic and thermostatic expansion valves are not suitable for the working capacities, a manually adjustable valve was used. The most critical point in the selection of the adjustment valve is the correct determination of the nozzle needle diameter. In addition, mini dryer was used in the system.

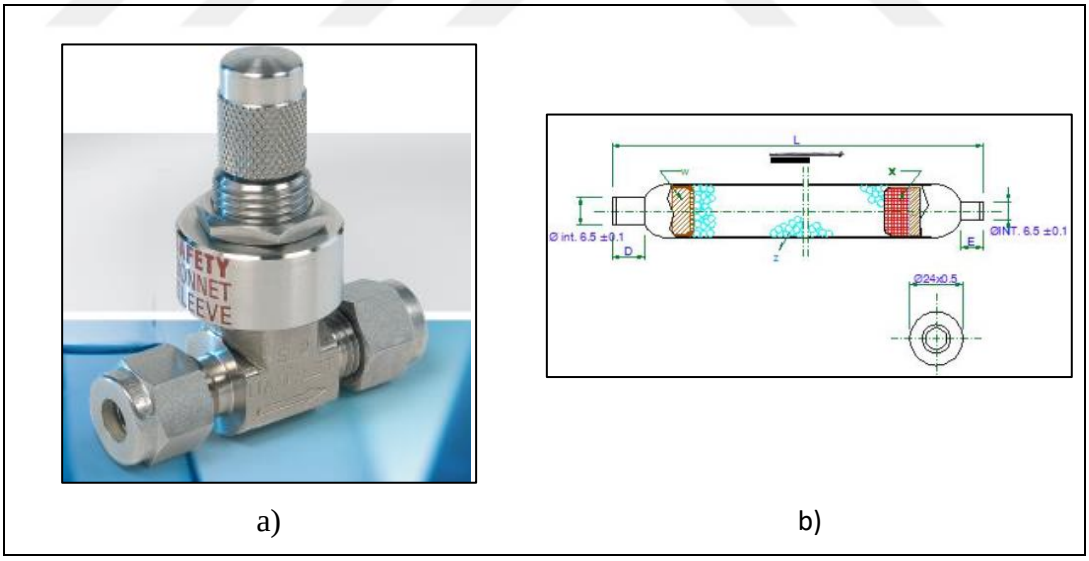

a) b)

Figure 4.5: a) Throttling valve, b) Dryer.

All sensors were connected 3 slot mainframe with built in RS232 interfaces data logger, Agilent 34970A. One slot with a module use for voltage signal from pressure transducers, two slot with two module use for thermocouples. Temperature and pressure measurements were collected a data acquisition system. The data is transferred to the computer where the test software is located. Thermocouples and pressure transducers properties are given Table 4.5.

a)

b)

Figure 4.6: a) Agilent 34970A data logger, b) Danfoss AKS 32R pressure transducer.

Table 4.5: Measurement devices.

Measurement	Instrument	Location	Range	Accuracy
Temperature	T Type Thermocouple	Surface temperature	-200 / 350 ºC	±0,3 ºC
Temperature	T Type Thermocouple	The refrigerant outlet temperature	-200 / 350 ºC	±0,3 ºC
Pressure	Danfoss AKS 32R	Evaporation pressure	-1 / 1200 kPa	±0,3%
Pressure	Danfoss AKS 32R	Evaporator inlet pressure	-1 / 1200 kPa	±0,3%
Pressure	Danfoss AKS 32R	Condenser outlet pressure	-1 / 3400 kPa	±0,3%

The calibration of equipment is important to check of sensor error. The thermocouples were calibrated a thermometer, FLUKE 9142 field metrology well, have with accuracy to ± 0,01 ºC.

The pressure transducers were calibration with a digital test manometer with pneumatic hand pump. Digital manometer supplies high accuracy ± 0,25 % and have -1 to 39 bar range.

The curve fit equations were determined for thermocouples and pressure transducers, the equations for sensors were entered data acquisition system. The sample calibration curves are given Figure 4.7, Figure 4.8 and Appendix A.

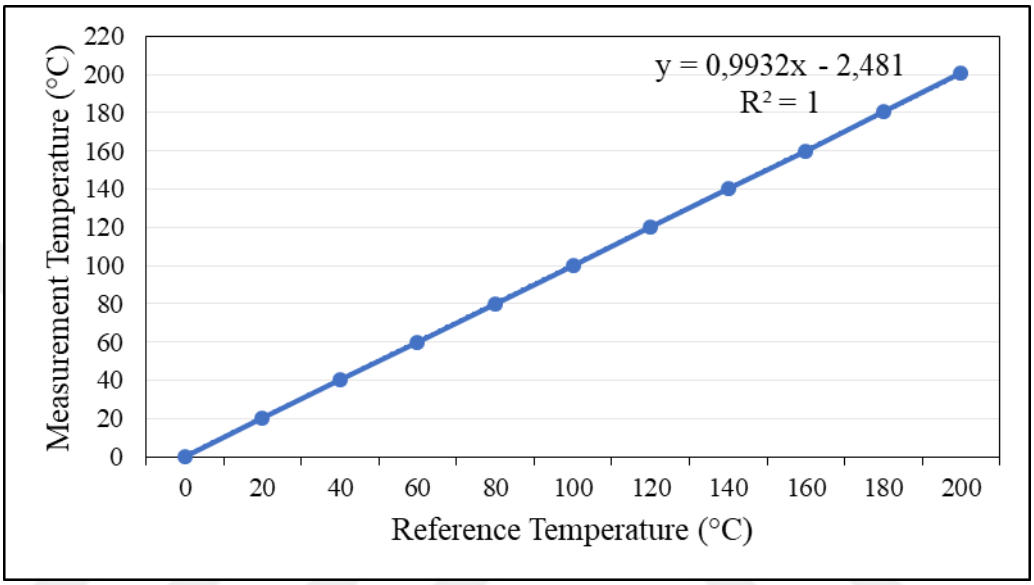

Figure 4.7: A sample calibration curve for thermocouple.

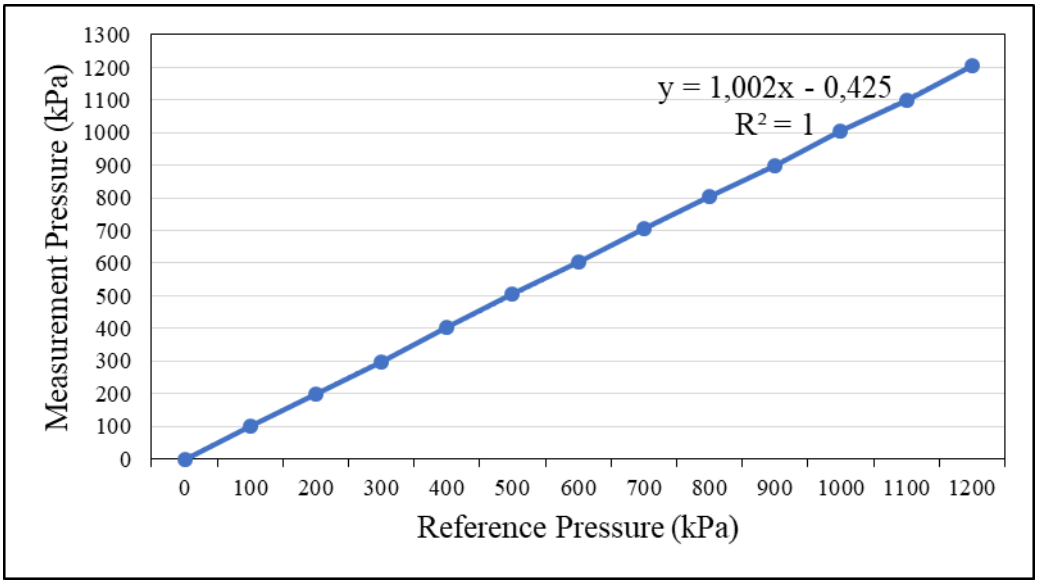

Figure 4.8: A sample calibration curve for pressure transducer.

The evaporator, designed and produced in the test section, was equipped with 200 mm x 200 mm silicon heaters that model electronic chips according to different heat loads, and the aluminum layer, 2 mm, was sequentially joined as shown in Figure 4.9 to measure the surface temperature. 16 T type thermocouples were fixed to the surface of the aluminum plate at the four point each pipe to read the surface temperatures. Two pressure transducer were connected inlet of evaporator and outlet of condenser, one T type thermocouple and one pressure transducer were connected outlet of evaporator for superheat and evaporation pressure. Totally, 20 channel data acquisition system, Agilent 34970A, was connected to the system and data were recorded Friterm Inc. Test Suite Software.

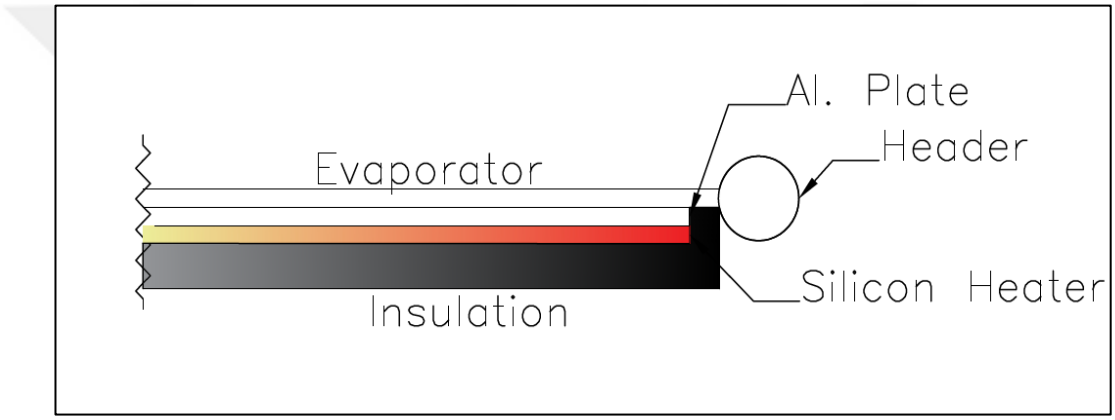

Figure 4.9: Test section illustration.

Sensors were connected to the required measuring points the test of minichannel evaporator designs. The superheat and subcooling values were adjusted by measuring the pressures and outlet temperatures of the evaporator and condenser. Silicone heaters with heat loads of 100 - 200 - 300 - 400 - 500 W, respectively, were prepared as in Figure 4.11 and taken to the test.

The test was carried out in the calorimetric test laboratory, located in the R&D center of Friterm Inc., in order not to be affected by any air flow. In addition, thermocouples, pressure transducer connection and data acquisition system were used here.

Figure 4.10: Test section view 1.

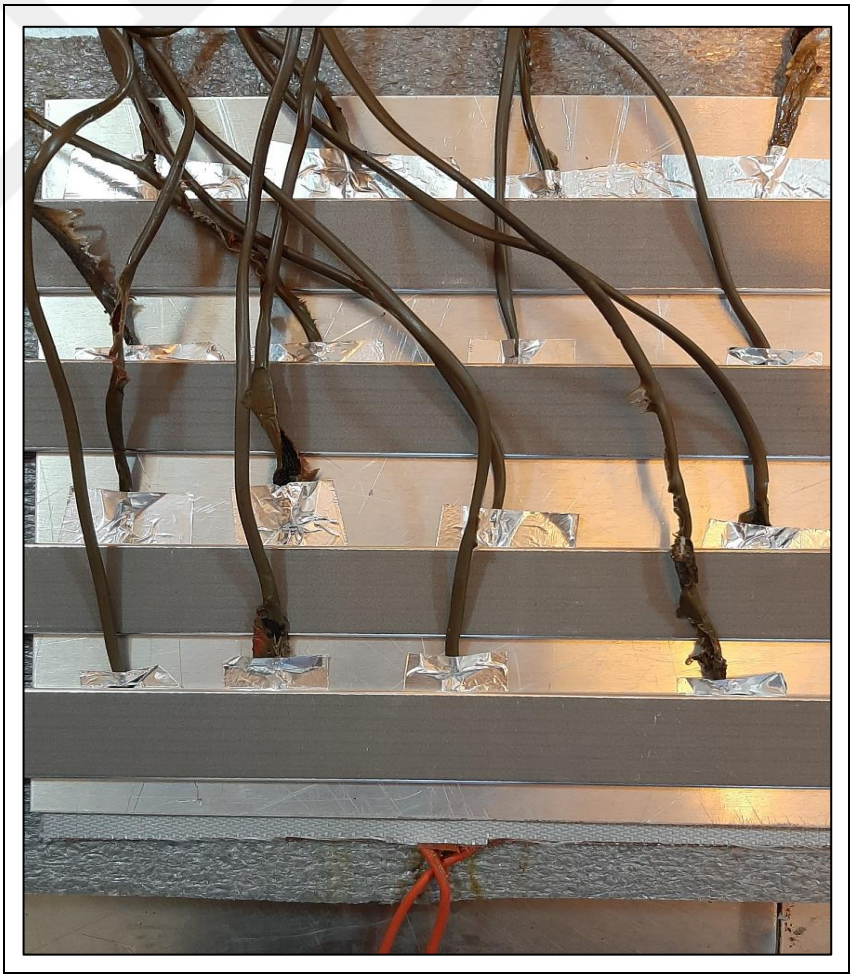

Figure 4.11: Test section view 2.

The test was started by running compressors and heaters at the same time. Necessary adjustments were made until the target approached the steady state condition. The condenser pressure and subcooling value were fixed by adjusting the EC fan speed. Evaporator pressure and superheat value were fixed by adjusting the throttling valve. After the test conditions were met in the cooling system, data recording was started. A temperature data was received per second. The average of the data received every thirty seconds was recorded.

5. RESULTS and DISCUSSION

It is very important that electronic circuits and boards of high-speed computers, military vehicles, etc. systems remain below the critical operating temperatures. If these critical temperatures are exceeded, electronic circuits will become inoperable. As a result, it seriously damages critical data loss and system security. Electronic circuits should not reach critical operating temperature, especially in order to prevent adverse conditions in military systems.

In this thesis, evaporator design was made for the vapor compression cooling system. Minichannel pipes used for evaporators were supplied from abroad as they are not manufactured in our country. For this reason, the standard pipes of the supplier was used. Evaporators were designed in two different circuit 60 and 48 (Table 5.1).

Table 5.1: Minichannel pipes specifications.

	Evaporator 1	**Evaporator 2**
Pipe Length	200 mm	200
Number of Pipe	5	4
Pipe Major Diameter	22 mm	22 mm
Pipe Minor Diameter	3 mm	3 mm
Pipe Wall Thickness	0.35 mm	0.35 mm
Pipe Channel Width	1.8 mm	1.8 mm
Number of Channel in Pipe	12	12
Total Circuit	60	48

Before the test process, the surface temperatures to be reached by the electronic circuits modeled of the evaporators designed for the cooling system operating conditions were determined. The effect of evaporation temperature, condensation temperature, superheat and subcooling values in the vapor compression cooling system was determined for both evaporators in the theoretically generated calculation module. Test conditions were tried to be applied after this comparison. In addition, evaporation temperature was determined as 5 ^{o}C in order to prevent freezing on evaporator surfaces that cool electronic circuits.

The Effect of Superheat; The effects of superheat on the evaporator design were investigated in cooling system operating conditions. For the working conditions given in Table 5.2, the performance of evaporator 1 in Figure 5.1 and evaporator 2 in Figure 5.2 are given.

Table 5.2: Superheat conditions.

Calculated Conditions	
Evaporator Temperature	5 °C
Condensing temperature	40 °C
Subcooling	1 K
Superheat	1 - 5 -10 K

According to the calculations, superheat increase causes the surface temperature to increase by 23%. There is an increase in the same trend in both evaporators. Under these operating conditions, the evaporator 1 stays safely up to 400 W up to 5 K superheat. Evaporator 2 was calculated to cool down to 82 °C with a heat load of only 200 W. It is inconvenient to use this design above this heat load. In Figure 5.3 and 5.4, it can be seen that the superheat increase increases the evaporator pressure loss.

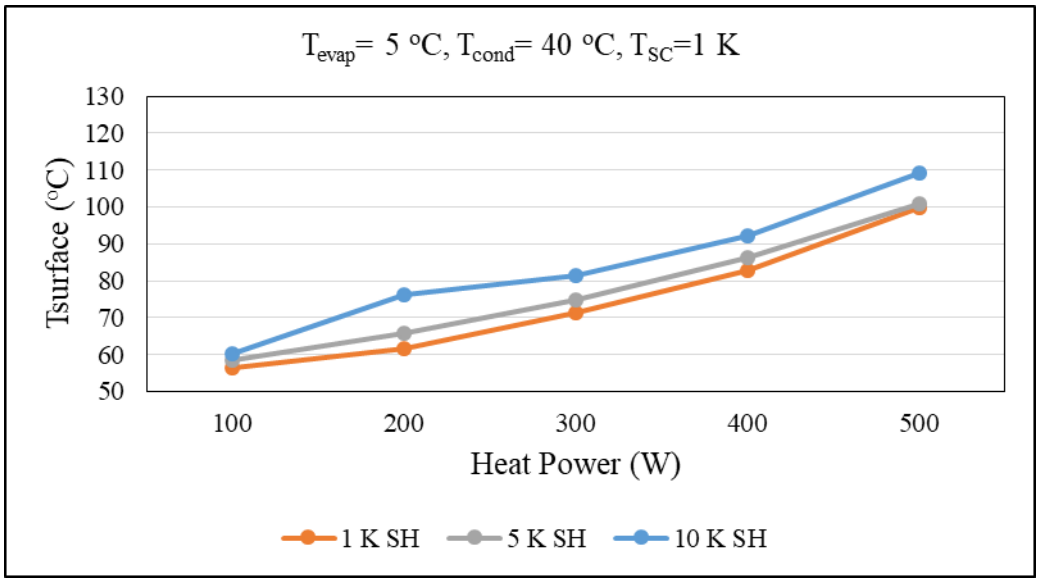

Figure 5.1: Superheat effect in evaporator 1.

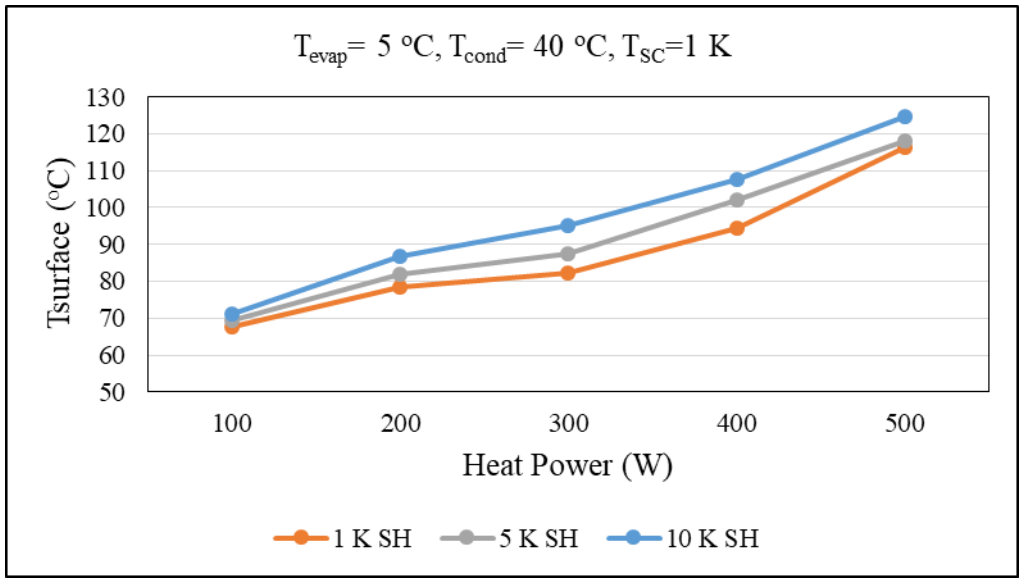

Figure 5.2: Superheat effect in evaporator 2.

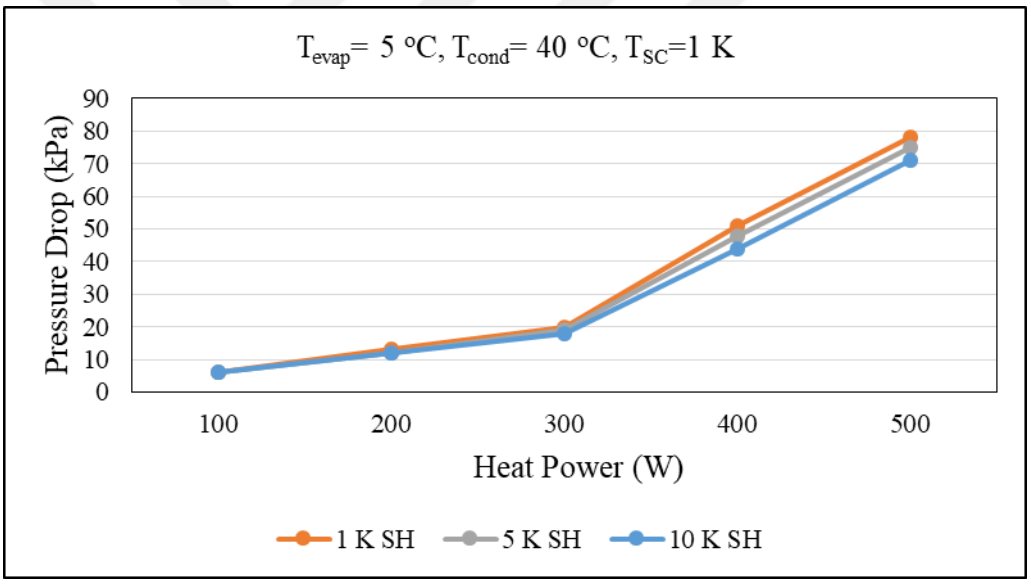

Figure 5.3: Pressure drop in evaporator 1.

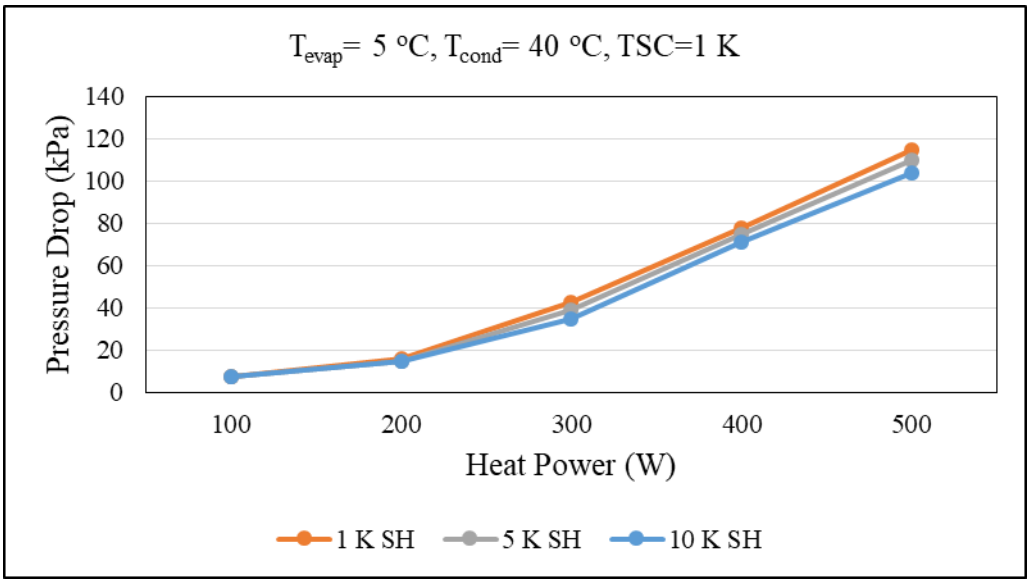

Figure 5.4: Pressure drop in evaporator 2.

The Effect of Condensation Temperatures; The effects of condensation temperatures on the evaporator design were investigated in cooling system operating conditions. For the working conditions given in Table 5.3, the performance of evaporator 1 in Figure 5.5 and evaporator 2 in Figure 5.6 are given. Pressure loss graphs are given in Appendix B.

Table 5.3: Condensation temperature conditions.

Calculated Conditions	
Evaporator Temperature	5 °C
Subcooling	1 K
Superheat	5 K
Condensing temperature	40 - 45 - 50 °C

When the figures are examined, the increase of the condenser temperature causes the surface temperature to increase. It was observed that the surface temperature for evaporator 1 at 400 W heat load exceeded 85 °C. For evaporator 2, the surface temperature increased up to 132 °C at a value above 200 W heat load. As can be seen from these results, evaporator designed at high condenser temperature should not be used.

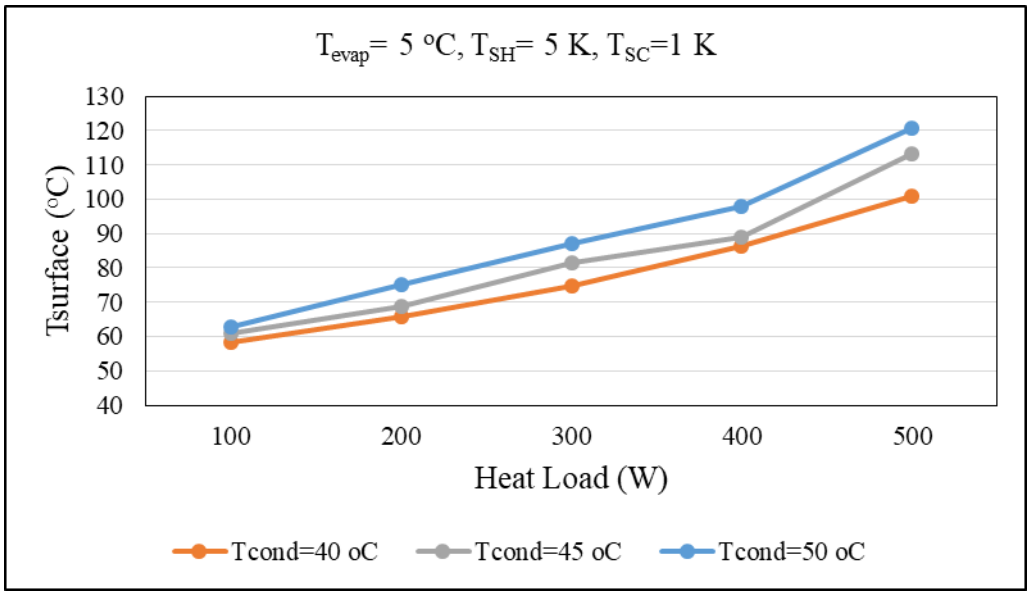

Figure 5.5: Condensation temperature effect in evaporator 1.

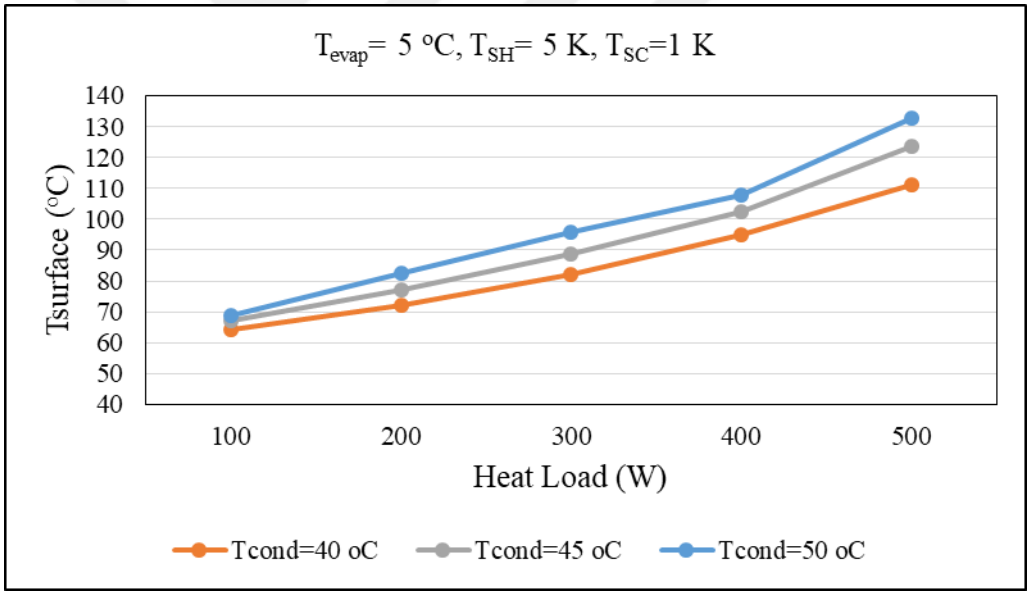

Figure 5.6: Condensation temperature effect in evaporator 2.

The Effect of Subcooling; The effects of subcooling on the evaporator design were investigated in cooling system operating conditions. For the working conditions given in Table 4.4, the performance of evaporator 1 in Figure 4.7 and evaporator 2 in Figure 4.8 are given. Pressure loss graphs are given in Appendix B.

Table 5.4: Subcooling conditions.

Calculated Conditions	
Evaporator Temperature	5 °C
Condensing temperature	40 °C
Superheat	5 K
Subcooling	1 - 5 -10 K

According to calculations, as the subcooling value increases, evaporator performance increases. Despite a 400 W heat load for the evaporator 1 under design conditions, the surface temperature at a value of 5 K was calculated to be 83 °C. Evaporator 2 performs better in subcooling increase compared to other conditions.

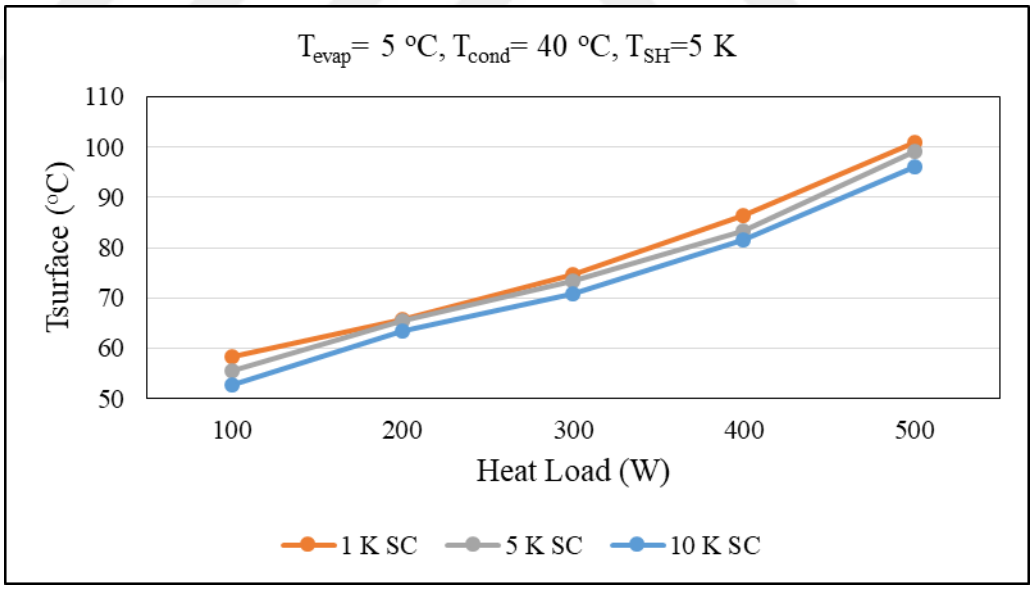

Figure 5.7: Subcooling effect in evaporator 1.

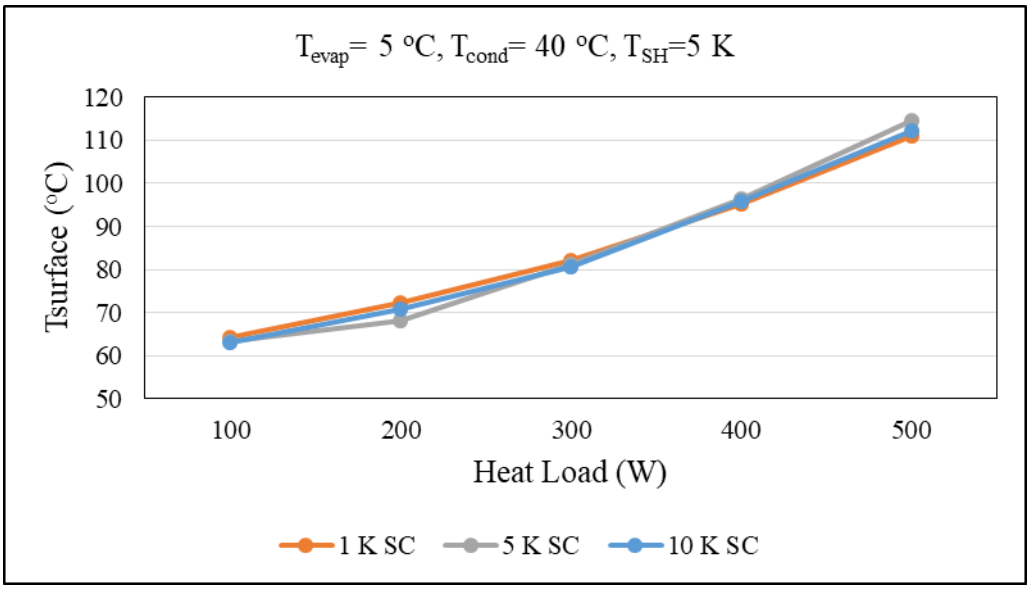

Figure 5.8: Subcooling effect in evaporator 2.

The Effect of Subcooling at 1 K Superheat; The effects of subcooling at low superheat value on the evaporator design were investigated in cooling system operating conditions. For the working conditions given in Table 5.5, the performance of evaporator 1 in Figure 5.9 and evaporator 2 in Figure 4.10 are given. Pressure loss graphs are given in Appendix B.

Table 5.5: Subcooling conditions at 1 K superheat.

Calculated Conditions	
Evaporator Temperature	5 °C
Condensing temperature	40 °C
Superheat	1 K
Subcooling	1 - 5 -10 K

The increase in evaporator performance can be seen in Figure 5.7 and Figure 5.8, with a subcooling effect at 5K superheat. The increase in superheat value affects the performance negatively. In these conditions, at low superheat and high subcooling value, the evaporator 1 was slightly improved. However, it is seen in Figure 5.9 that there is not much difference in 500 W heat power. It can be seen here that the evaporator 2 performance is not sufficient.

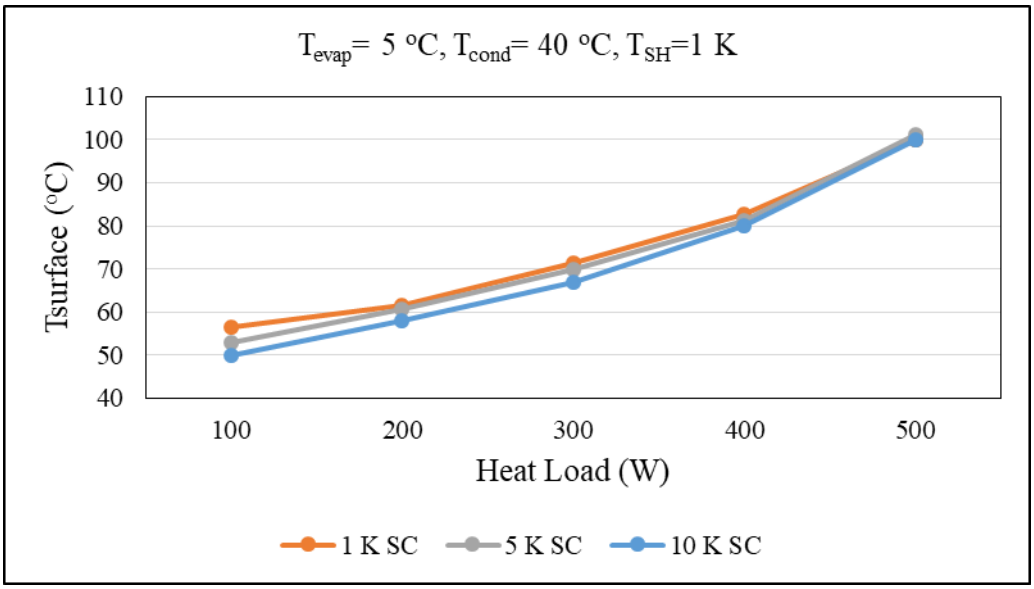

Figure 5.9: Subcooling effect at 1 K superheat in evaporator 1.

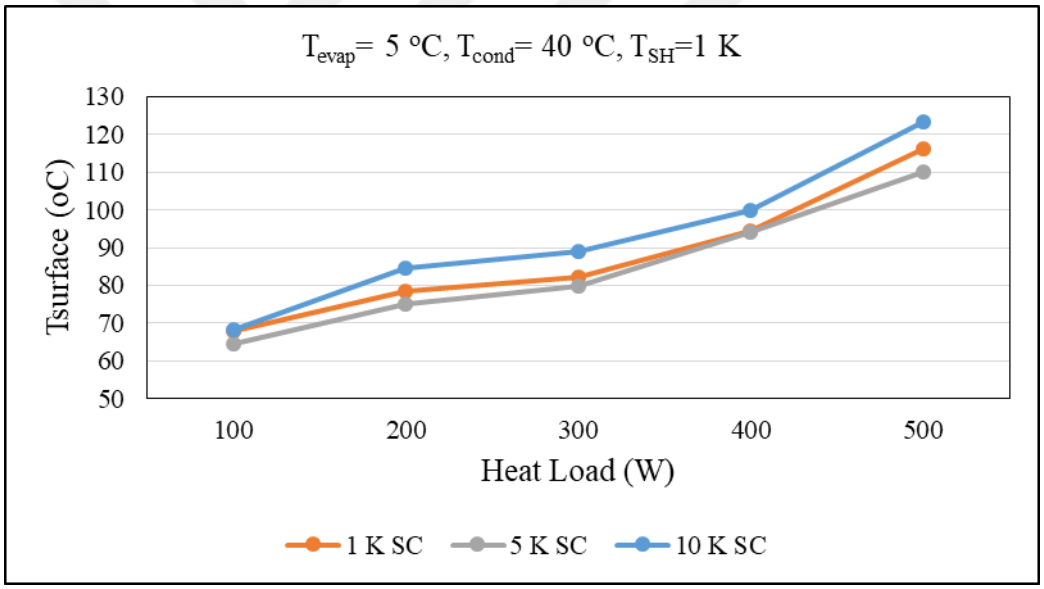

Figure 5.10: Subcooling effect at 1 K superheat in evaporator 2.

In the calculation module for the evaporator performances studied in theory, the working conditions in different scenarios were examined. Test conditions were determined according to these results and the operating regimes of the devices. Low superheat and subcooling values were chosen for the tests. For comparisons, the same operating conditions were selected for all tests. Selected conditions and stable working conditions for all test are given Table 5.6.

Table 5.6: Selected and stable working conditions.

	Selected conditions	Stable Working Conditions
Evaporation Temperature/Pressure	5 ^{o}C/250 kPa	5,3 ^{o}C/252 kPa
Superheat	5 K	5-6 K
Condensing Temperature/Pressure	40 ^{o}C/915 kPa	38 ^{o}C/862 kPa
Subcooling	1 K	2-3 K

Test results were started to be taken when the cooling system reaches equilibrium under specified operating conditions (Appendix C). The comparison of the surface temperature calculated and final temperatures from test results for the selected conditions are given in Table 5.7.

Table 5.7: Comparison of the surface temperatures.

	Evaporator 1			Evaporator 2		
Heat Load (W)	Calculation (^{o}C)	Test Result (^{o}C)	Temperature Rate %	Calculation (^{o}C)	Test Result (^{o}C)	Temperature Rate %
100	58,33	59,00	1,15	69,23	71,59	3,41
200	65,69	66,94	1,91	81,93	82,70	0,94
300	74,77	75,51	0,99	87,58	82,30	-6,03
400	86,46	84,37	-2,42	102,22	99,16	-3,00
500	100,94	101,52	0,57	117,99	120,68	2,28

During this time, the temperature of the measuring points increased according to heat load given. Temperature changes depending on time are given in Figures 5.11 and 5.12. The last value is the value at which the temperature was constant. It has been seen in tests that the evaporator 1 can be used safely up to 400 W. The surface temperature of the electronic circuit, modeled at a 400 W heat load, remained below 85 ºC. However, the evaporator 2 does not perform so well. Also, calculations confirm this. There is a maximum difference of 6% between test results and calculations. This corresponds to a difference of 6 - 7 ºC.

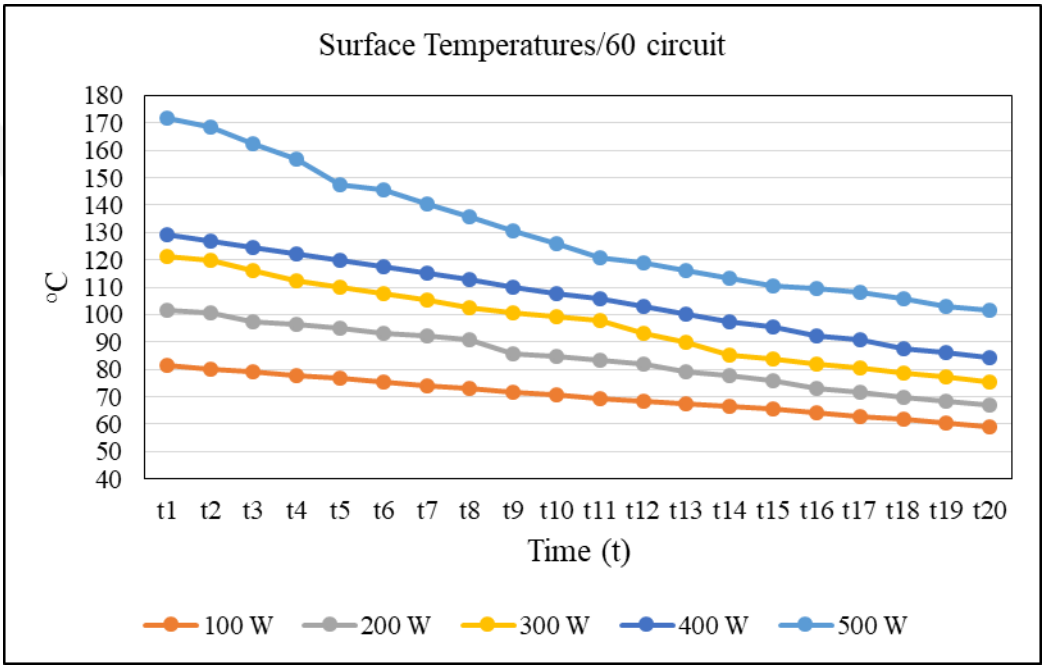

Figure 5.11: Temperature changes depending on time for evaporator 1.

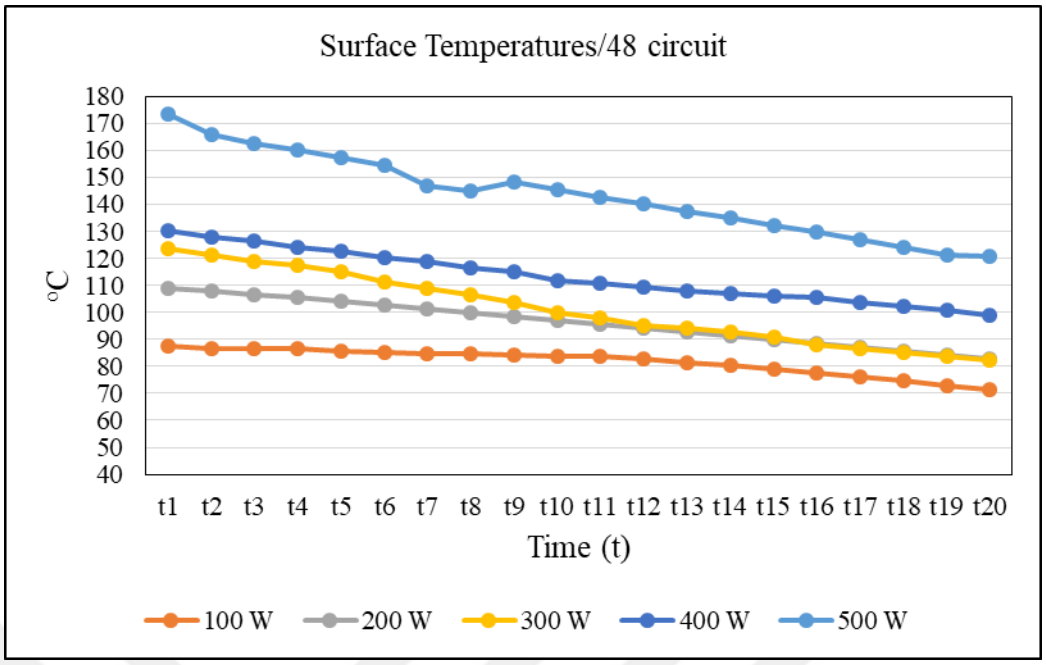

Figure 5.12: Temperature changes depending on time for evaporator 2.

The change of calculated vapor quality along to evaporator length for working condition is given in Figure 5.13. The input vapor quality calculated according to the working condition is 0,247. It is calculated vapor quality as 1,024 at 5 K superheat value from the output enthalpy of the refrigerant. In this case, most of the heat transfer in the evaporators takes place in two phase region.

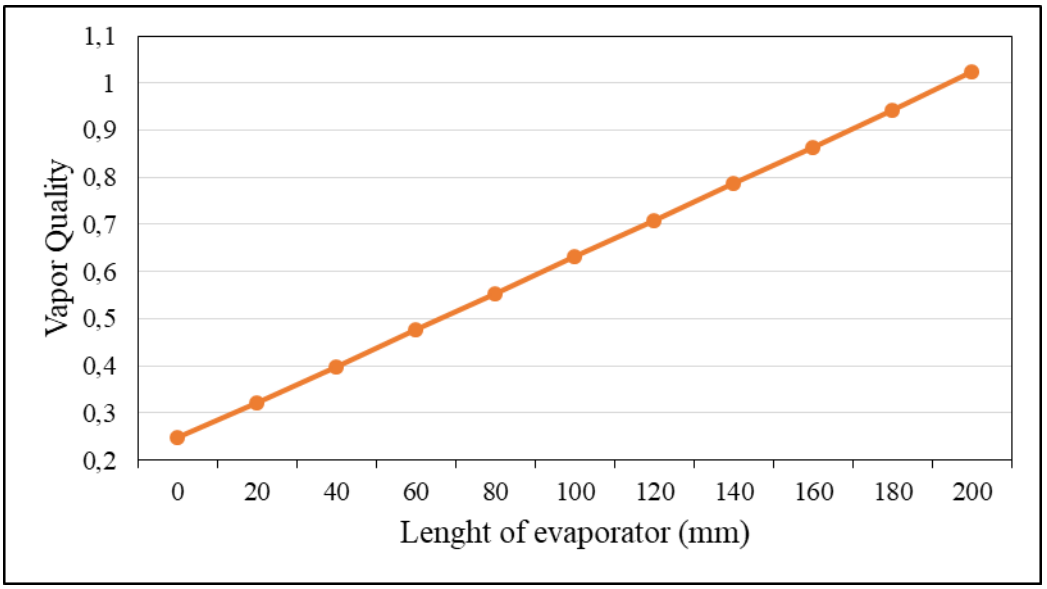

Figure 5.13: Change of vapor quality along to evaporator length.

The variation figures of the two phase heat transfer coefficient in the evaporators for each heat load are given below. The inlet vapor quality of the refrigerant taken from the calculation module is shown on the graphs. In all calculations, the evaporator inlet vapor quality is the same value. In the calculation module does not calculate heat transfer coefficient before diffraction on Figure 5.14, 5.15, 5.16, 5.17, 5.18. The peak point of the heat transfer coefficient in the two phase regions is between 0.3 and 0.4, and this can be explained according to the flow regime. The flow has nucleating bubbles at the minichannels walls. In this region, trend of HTC almost constant to calculated. As expected, the heat transfer coefficient decreases until full evaporation of the refrigerant in the minichannels. HTC in evaporator 1 rate is smaller 20% than HTC in evaporator 2 for all heat load because hydraulic diameter. In Figure 5.17 and 5.18, 100 W and 200W heat load of designed evaporators have low mass flow, so low mass flow show that evaporation for refrigerant goes from bubble flow to annular flow directly.

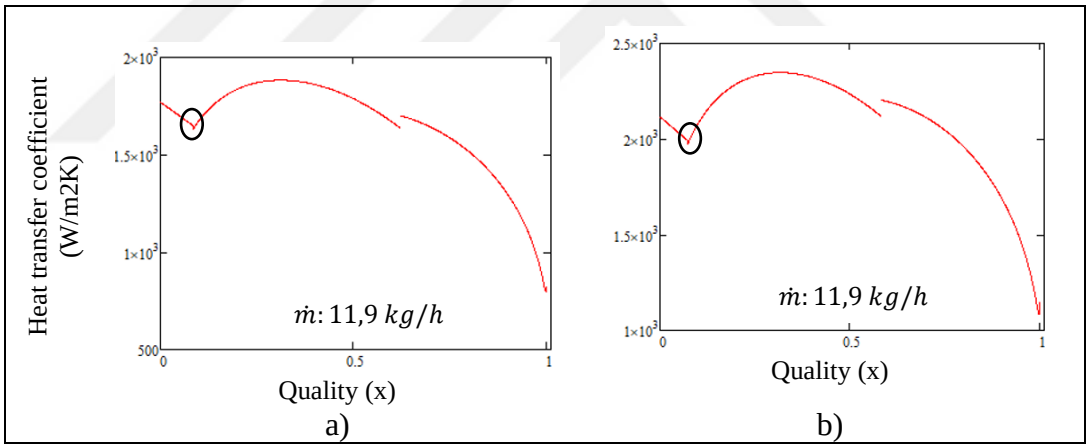

Figure 5.14: a) Two phase HTC in evaporator 1 at 500 W, b) Two phase HTC in evaporator 2 at 500 W.

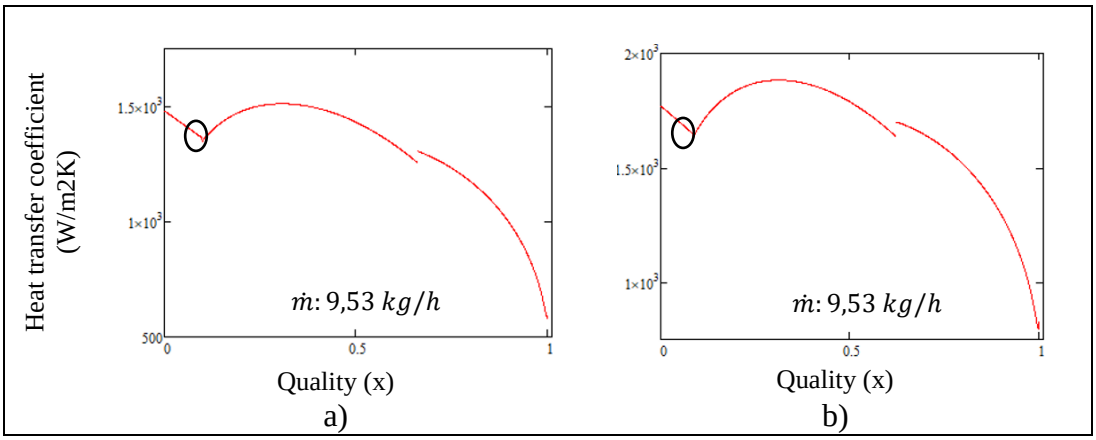

Figure 5.15: a) Two phase HTC in evaporator 1 at 400 W, b) Two phase HTC in evaporator 2 at 400 W.

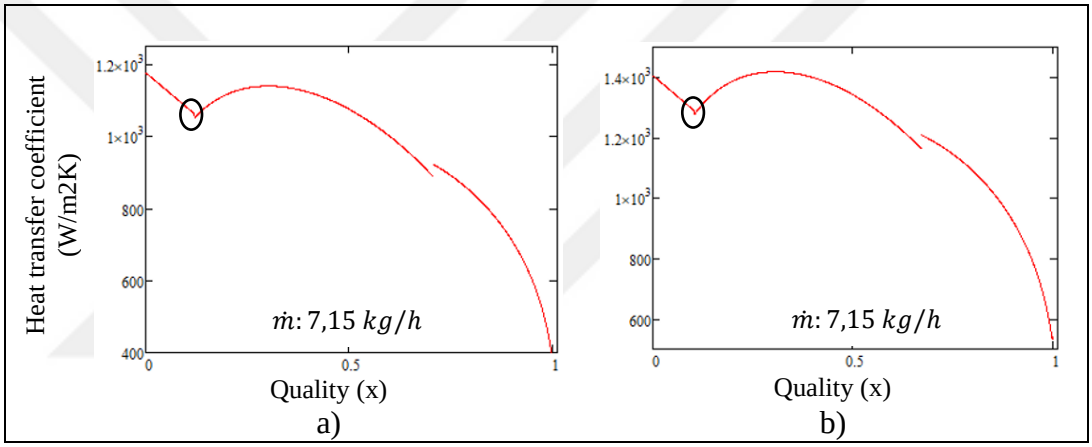

Figure 5.16: a) Two phase HTC in evaporator 1 at 300 W, b) Two phase HTC in evaporator 2 at 300 W.

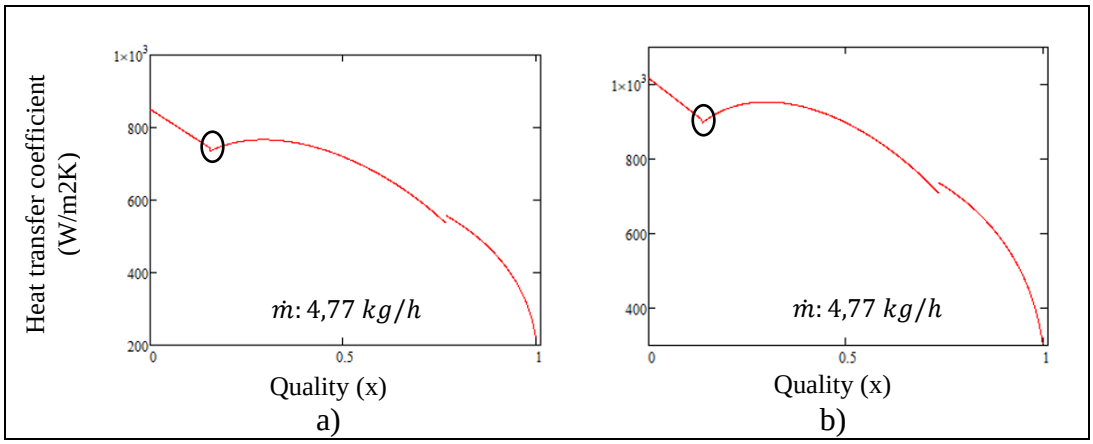

Figure 5.17: a) Two phase HTC in evaporator 1 at 200 W, b) Two phase HTC in evaporator 2 at 200 W.

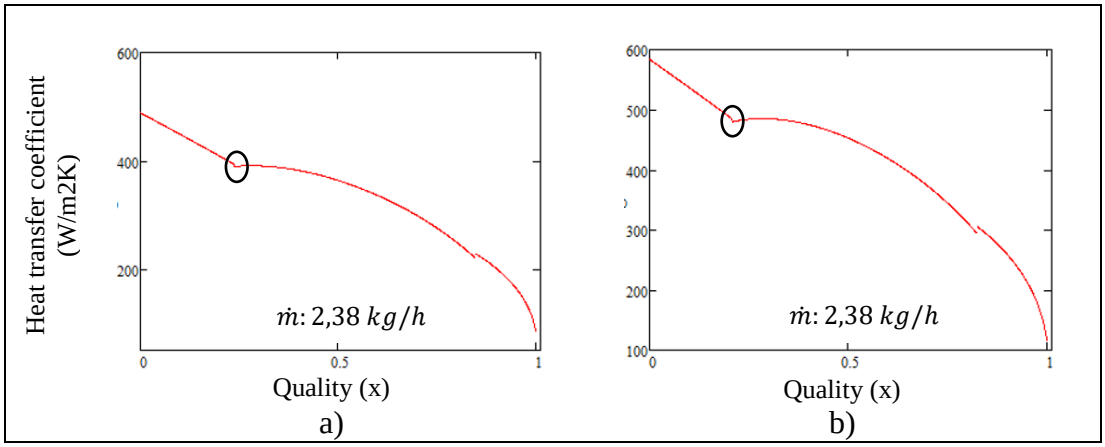

Figure 5.18: a) Two phase HTC in evaporator 1 at 100 W, b) Two phase HTC in evaporator 2 at 100 W.

The HTC values at two phase region and single phase region in evaporators are given Table 5.8. The single phase is defined as vapor region. The vapor quality at 1 to 1,024 depends on mass flow and heat load.

Table 5.8: The HTC values for evaporator 1 and evaporator 2.

	Evaporator 1		**Evaporator 2**	
Heat Load (W)	HTC Two phase (W/m^2K)	HTC Single phase (W/m^2K)	HTC Two phase (W/m^2K)	HTC Single phase (W/m^2K)
100	853	26,72	1066	27,39
200	1149	29,43	1437	30,77
300	1408	32,21	1760	49,15
400	1625	56,21	2032	85,93
500	1817	85,75	2272	114,86

Following the comparison between the heat transfer coefficients the evaporator is also evaluated for the pressure drop. The pressure drop values are measured with the pressure transducers the pressure drop between the inlet and outlet pressure values at the evaporators. In the evaporator pressure drop, up to 40% deviations were observed between calculations and test results (Figure 5.19 and Figure 5.20).

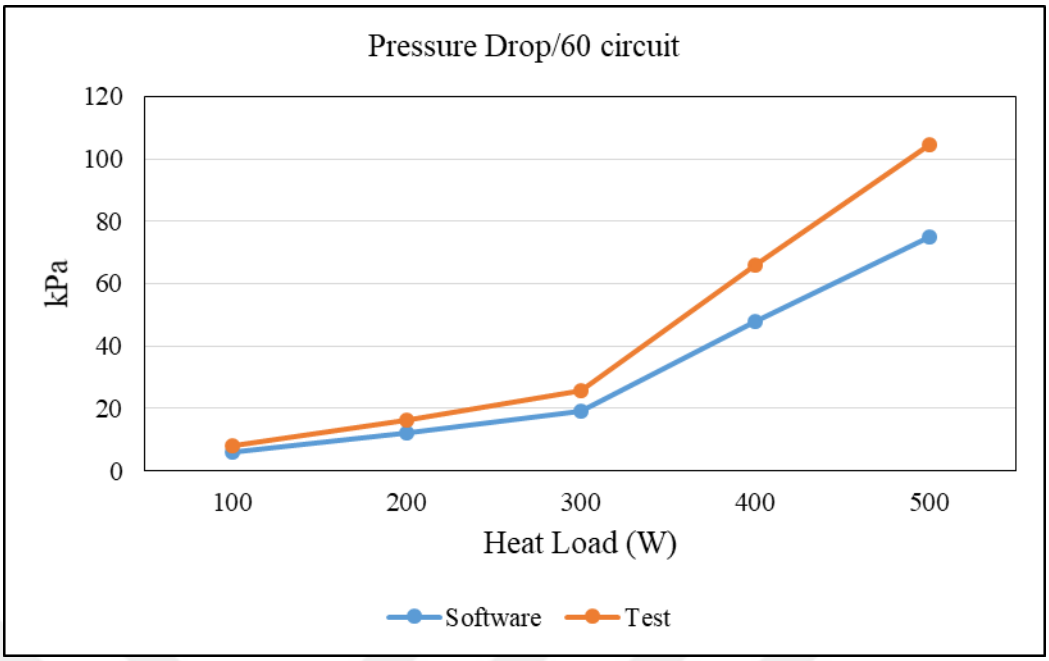

Figure 5.19: Pressure drop for evaporator 1.

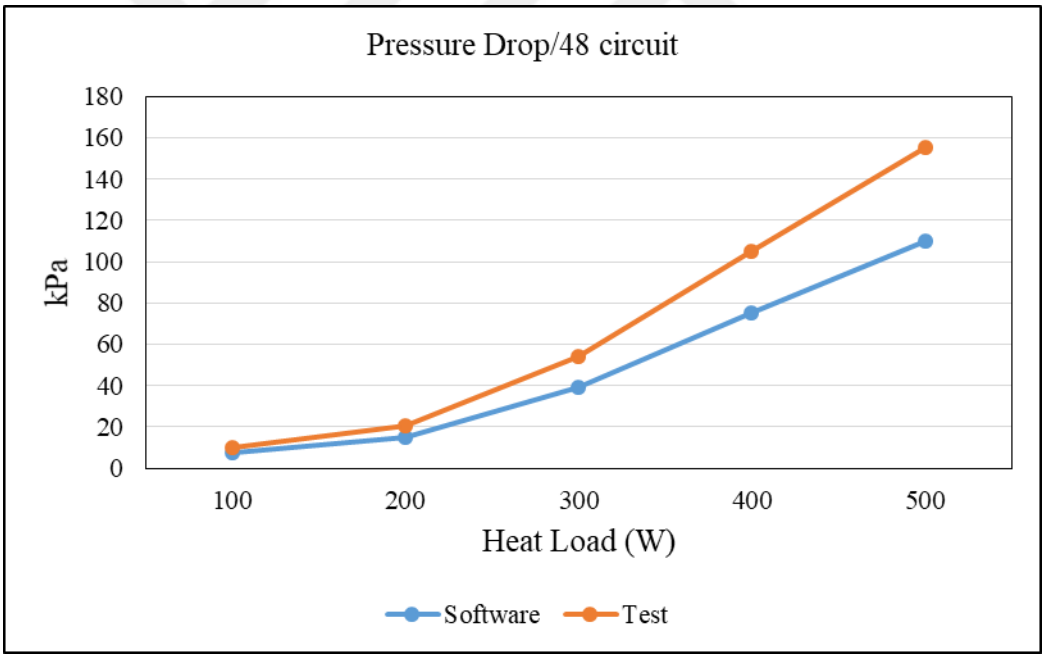

Figure 5.20: Pressure drop for evaporator 2.

Cooling systems are very important for the safety of electronic devices. Critical temperature values should not be exceeded for device safety. For this reason, passive and active cooling techniques, which are customized according to electronic cooling packages, are used. These cooling techniques are inadequate in some cases. Therefore, vapor compression refrigeration cycles can be preferred for the system. The most important component in a vapor compression refrigeration cycle is the evaporator. Evaporator performance is especially important for keeping electronics below critical temperature.

Although there are many studies in the literature and in the market, minichannel evaporator is not used much. More evaporator designs are available with conventional circular tubes. In this thesis study, minichannel evaporator designs were made and cooling performances were tested. Evaporators have performed very well at a high heat load for high electronic components. It is especially suitable to use evaporator 1 at high heat load. There is not much difference between test results and the outputs of the calculation module created for minichannel evaporator design. In this calculation module, electronic cooling units with different designs can be calculated. This thesis study will be the beginning of many studies planned for the future. The future studies are listed as below.

- Since the pressure loss difference between design and test is high, the pressure difference correlations in the literature will be investigated and used in detail.
- The vapor compression cycle designed for electronic cooling will be handled as a whole and the coefficient of performance will be examined.
- The evaporator will be designed to focus on flow regime in minichannels.
- Minichannel types used in evaporator design will be changed and flow distribution in header will be examined.
- The compressor used in the system will be replaced with a mini compressor.
- The performance test of the minichannel condenser used in the system will be performed in detail. The condenser inlet air temperature will be checked. The air temperature will be regulated and tested to cool the electronics of military vehicles operating at high temperatures and difficult conditions.
- A new evaporator design will be made for high heat loads.

REFERENCES

[1] Arden W., Cogez P., Graef M., Goltz G., (2005), "Internatıonal Technology Roadmap for Semiconductors", 2005 Edition, Semiconductor Industry Association.

[2] Cogez P., Graef M., Huizing B., Mahnkopf R., (2013), "Internatıonal Technology Roadmap for Semiconductors", 2013 Edition, Semiconductor Industry Association.

[3] Graef M., Huizing B., Mahnkopf R., (2015), "Internatıonal Technology Roadmap for Semıconductors", 2015 Edition, Semiconductor Industry Association.

[4] Graef M., Huizing B., Mahnkopf R., (2006), "Internatıonal Technology Roadmap for Semıconductors", 2006 Edition, Semiconductor Industry Association.

[5] Pfahl R. C., McElroy J., (2005), "The 2004 International Electronics Manufacturing Initiative (iNEMI) Technology Roadmaps", Institute of Electric and Electronics Engineers Conference, 0-7803-9292-2, Shanghai, China, 27-29 June.

[6] Agostini B., Fabbri M., Park J. E., Wojtan L., Thome J. R., Michel B., (2007), "State of the Art of High Heat Flux Cooling Technologies", Heat Transfer Engineering, 28 (4), 258-281.

[7] MIL-HDBK-217F, (1991), "Reliability Prediction of Electronic Equipment, Military Handbook", USA Department of Defense.

[8] Murshed S. M., Nieto de Castro C. A., (2017), "A Critical Review of Traditional and Emerging Techniques and Fluids For Electronics Cooling", Renewable and Sustainable Energy Reviews, 78, 821-833.

[9] Ulrich R. K., (2006), "Advanced Electronic Packaging", 2nd Edition, John Wiley & Sons.

[10] Bar-Shalom D., (1989), "Altitude Effects on Heat Transfer Processes in Aircraft Electronic Equipment Cooling", Master Thesis, Massachusetts Institute of Technology.

[11] Scott W.A., (1974), "Cooling of Electronic Equipment", John Wiley and Sons.

[12] Murshed S. M., Nieto de Castro C. A., (2017), "A Critical Review of Traditional and Emerging Techniques and Fluids For Electronics Cooling", Renewable and Sustainable Energy Reviews, 78, 821-833.

[13] Regulation (EU) of The European Parliament and of the Council, (2014), On Fluorinated Greenhouse Gases and Repealing Regulation (EC), 517/2014-842/2006, 195-230.

[14] Çengel Y., (2011), "Heat and Mass Transfer", 1st edition, McGraw Hill.

[15] Fang X., Wu Q., Yuan Y., (2017), "A general correlation for saturated flow boiling heat transfer in channels of various sizes and flow directions", International Journal of Heat and Mass Transfer, 107, 972–981.

[16] Shah M. M., (2017), "Unified correlation for heat transfer during boiling in plain mini/micro and conventional channels", International Journal of Refrigeration, 74, 606-626.

[17] Satish G. K., (1999), "Handbook of Phase Change: Boiling and Condensation", 1st Edition, Taylor & Francis Group.

[18] Gnielinski V., (2013), "On heat transfer in tubes", International Journal of Heat and Mass Transfer, 63 (3), 134-140.

[19] Stephan P., Kabelac S., Kind M., Martin H., Mewes D., Schaber K., (2010), "VDI Heat Atlas", 2nd Edition, Springer.

[20] Poachaiyapoom A., Leardkun R., Mounkong J., Wongwises S., (2019), "Miniature vapor compression refrigeration system for electronics cooling", Case Studies in Thermal Engineering, 13, 100365.

[21] Wiriyasart S., Hommalee C., Naphon P., (2019), "Thermal cooling enhancement of dual processors computer with thermoelectric air cooler module", Case Studies in Thermal Engineering, 14, 100445.

[22] Ribeiro G., Barbosa J., Prata A., (2010), "Minichannel evaporator/heat pipe assembly for a chip cooling vapor compression refrigeration system", International Journal of Refrigeration, 33, 1402-1412.

[23] Mancin S., Zilio C., Righetti G., Rossetto L., (2013), "Mini vapor cycle system for high density electronic cooling applications", International Journal of Refrigeration, 36, 1191-1202.

[24] Wu Z., Du R., (2011), "Design and experimental study of a miniature vapor compression refrigeration system for electronics cooling", Applied Thermal Engineering, 31, 385-390.

[25] Bash C.E., (2001), "Analysis of Refrigerated Loops for Electronics Cooling, Proceeding of IPACK'01", The Pacific Rim/ASME International Electronic Packaging Technical Conference and Exhibition, 811-819.

[26] Zilio C., Righetti G., Mancin S., (2018), "Active and passive cooling technologies for thermal management of avionics in helicopters: Loop heat pipes and mini-Vapor Cycle System", Thermal Science and Engineering Progress, 5, 107-116.

[27] Lee J., Mudawar I., (2006), “Implementation of microchannel evaporator for high-heat-flux refrigeration cooling applications”, Transactions of the ASME, Vol.128, 30-37.

[28] Trutassanawin S., Groll E.A., Grimella S.V., Cremaschi L., (2006), “Experimental investigation of a miniature scale refrigeration system for electronics cooling”, Purdue e-Pubs – CTRC Cooling Technologies Research Center, 135.

[29] Churchill SW., (1977), “Friction factor equations spans all fluid-flow regimes”, Journal of Chemical Engineering, 84(24), 91-92.

[30] Shah R. K., (2003), “Heat Exchanger Design” , 1st edition, John Wiley and Sons.

[31] Shah M. M., (2017), “A Correlation for Heat Transfer During Boiling on Bundles of Horizontal Plain and Enhanced Tubes”, International Journal of Refrigeration, 78, 47-59.

[32] Heck M. S., (1986), “Frictional Pressure Drop for Gas Liquid Flow in Horizontal Pipelines”, 9th Australasian Fluid Mechanics Conference, 395-399, Auckland, 8-12 December.

BIOGRAPHY

Mehmet Harun Sökücü was born in Gaziantep, 26 February 1989. After he had graduated from Gaziantep Anatolian High School, took the Bachelor's Degree from Yalova University Department of Energy Systems Engineering in 2016. He started graduate school at Gebze Technical University, Graduate School of Natural and Applied Sciences Department of Mechanical Engineering. He has been working at Friterm Termik Cihazlar A.Ş. as a Laboratuary and Test Engineer at R&D department.

APPENDICES

Appendix A: The Time Dependent of Thermocouple Calibrations

Table A1.1: Calibration data for thermocouples.

Time (s)	TC_{ref} (°C)	TC #1 (°C)	TC #2 (°C)	TC #3 (°C)	TC #4 (°C)	TC #5 (°C)	TC #6 (°C)	TC #7 (°C)	TC #8 (°C)	TC #9 (°C)	TC #10 (°C)	TC #11 (°C)	TC #12 (°C)	TC #13 (°C)	TC #14 (°C)	TC #15 (°C)
10	23,6	23,6	23,5	23,4	23,4	23,7	23,6	23,4	23,6	23,4	23,5	23,4	23,3	23,4	23,5	23,3
20	23,6	23,5	23,6	23,5	23,6	23,5	23,5	23,5	23,6	23,6	23,5	23,4	23,3	23,5	23,5	23,3
30	23,6	23,6	23,6	23,5	23,4	23,6	23,6	23,6	23,7	23,5	23,5	23,5	23,4	23,5	23,5	23,4
40	23,7	23,7	23,6	23,5	23,6	23,7	23,6	23,5	23,6	23,5	23,6	23,6	23,4	23,5	23,6	23,3
50	23,7	23,7	23,7	23,5	23,5	23,6	23,6	23,6	23,7	23,6	23,5	23,5	23,4	23,6	23,6	23,4
60	23,8	23,7	23,8	23,7	23,6	23,7	23,6	23,6	23,6	23,4	23,5	23,5	23,4	23,6	23,6	23,4
70	23,8	23,7	23,8	23,7	23,6	23,6	23,7	23,6	23,7	23,5	23,7	23,6	23,5	23,5	23,8	23,4
80	23,8	23,7	23,8	23,8	23,5	23,7	23,6	23,7	23,6	23,5	23,6	23,6	23,5	23,6	23,6	23,5
90	23,7	23,8	23,8	23,8	23,6	23,8	23,7	23,6	23,9	23,4	23,6	23,6	23,5	23,7	23,7	23,4
100	23,8	23,8	23,8	23,8	23,7	23,8	23,7	23,6	23,7	23,6	23,7	23,6	23,5	23,6	23,8	23,5
110	23,8	23,9	23,8	23,8	23,7	23,8	23,6	23,7	23,6	23,4	23,7	23,7	23,6	23,7	23,8	23,5
120	23,9	23,9	23,9	23,8	23,7	23,8	23,7	23,7	23,9	23,5	23,7	23,6	23,6	23,6	23,7	23,5
130	23,9	23,9	23,9	23,9	23,6	23,8	23,8	23,7	23,8	23,5	23,7	23,6	23,6	23,7	23,8	23,6
140	23,9	23,9	23,9	23,9	23,6	23,9	23,6	23,8	23,8	23,7	23,8	23,7	23,6	23,6	23,7	23,6
150	24,0	24,0	23,9	24,0	23,7	23,9	23,7	23,7	23,7	23,6	23,8	23,8	23,6	23,8	23,9	23,6
160	23,9	23,9	24,0	24,0	23,8	23,8	23,7	23,6	23,6	23,5	23,7	23,6	23,6	23,8	23,8	23,6
170	23,9	24,0	23,9	24,0	23,8	23,9	23,8	23,7	23,8	23,6	23,8	23,8	23,6	23,8	23,7	23,6
180	24,0	23,9	24,0	24,1	23,9	23,9	23,8	23,7	23,9	23,6	23,8	23,8	23,6	23,8	23,7	23,6
190	24,0	24,0	24,1	24,0	23,9	24,0	23,9	23,7	23,8	23,6	23,8	23,8	23,7	23,8	23,9	23,6
200	24,0	24,0	24,1	24,1	23,9	24,0	23,8	23,8	23,9	23,6	23,8	23,8	23,7	23,8	23,9	23,7
210	24,0	24,0	24,0	24,0	23,9	24,0	23,8	23,7	23,8	23,7	23,8	23,9	23,7	23,8	24,0	23,6
220	24,1	24,1	24,1	24,0	23,9	23,9	23,8	23,7	23,9	23,7	23,8	23,8	23,8	23,8	24,0	23,8
230	24,1	24,1	24,2	24,1	24,0	24,0	23,8	23,8	23,8	23,8	23,9	23,9	23,8	23,9	23,9	23,8
240	24,2	24,1	24,2	24,2	24,0	24,0	23,9	23,7	23,8	23,8	23,9	23,9	23,8	23,9	24,0	23,8
250	24,2	24,1	24,1	24,2	24,0	24,1	23,9	23,8	23,9	23,8	24,0	23,9	23,8	24,0	23,9	23,8
260	24,2	24,1	24,2	24,2	24,0	24,0	24,0	23,9	23,9	23,8	24,0	24,0	23,9	24,0	24,1	23,8
270	24,1	24,1	24,0	24,2	24,0	23,9	24,0	23,8	23,9	23,9	24,0	23,8	24,0	24,0	24,0	23,8
280	24,1	24,1	24,0	24,2	24,0	24,0	24,1	24,0	24,1	24,0	24,0	23,8	24,1	24,1	24,2	24,0
290	24,2	24,1	24,1	24,2	24,1	24,1	24,2	24,1	24,1	24,0	24,1	23,9	24,0	24,0	24,1	24,3
300	24,2	24,2	24,1	24,2	24,2	24,0	24,3	24,1	24,1	24,0	24,0	24,0	24,2	24,0	24,2	24,3

Time (s)	TC_{ref} (°C)	TC_{outlet} (°C)
10	22,1	22,3
20	22,2	22,2
30	22,1	22,2
40	22,1	22,1
50	22,2	22,1
60	22,1	22,2
70	22,2	22,4
80	22,2	22,2
90	22,1	22,2
100	22,2	22,4
110	22,2	22,3
120	22,2	22,3
130	22,2	22,2
140	22,4	22,4
150	22,3	22,5
160	22,2	22,5
170	22,3	22,4
180	22,3	22,5
190	22,5	22,5
200	22,5	22,4
210	22,4	22,4
220	22,5	22,5
230	22,4	22,5
240	22,4	22,7
250	22,5	22,5
260	22,6	22,7
270	22,4	22,3
280	22,5	22,3
290	22,4	22,4
300	22,6	22,5

Appendix B: Pressure Drop Tables

- The Effect of Condensation Temperatures at Pressure Drop

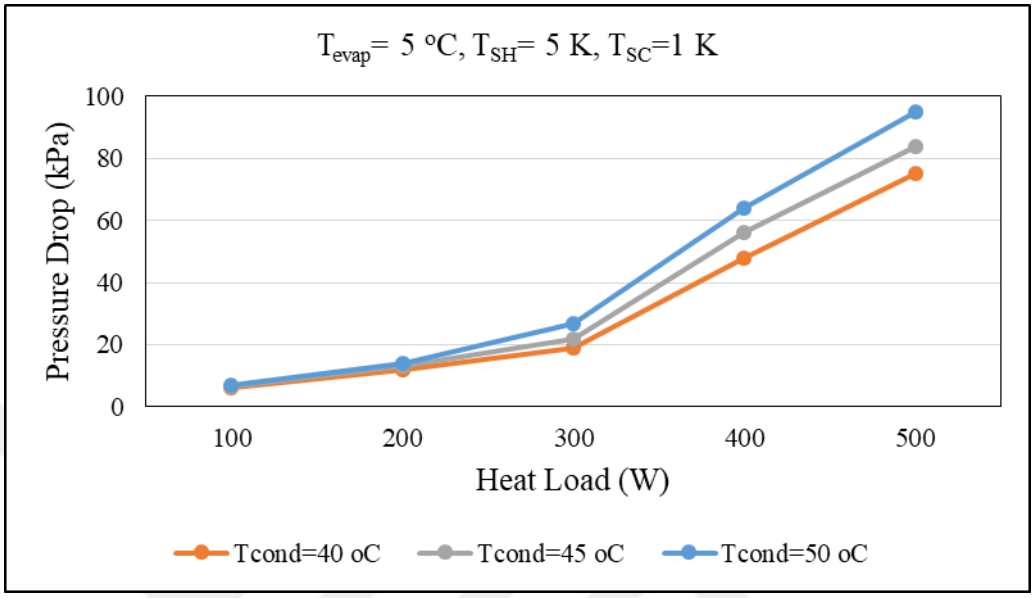

Figure B1.1: Pressure drop in evaporator 1.

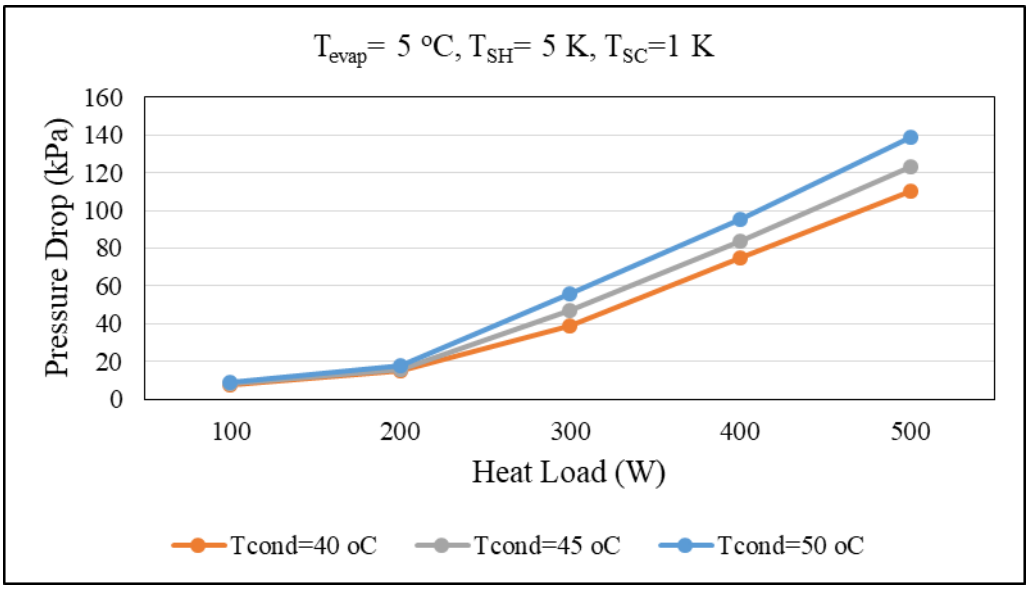

Figure B1.2: Pressure drop in evaporator 2.

- The Effect of Subcooling

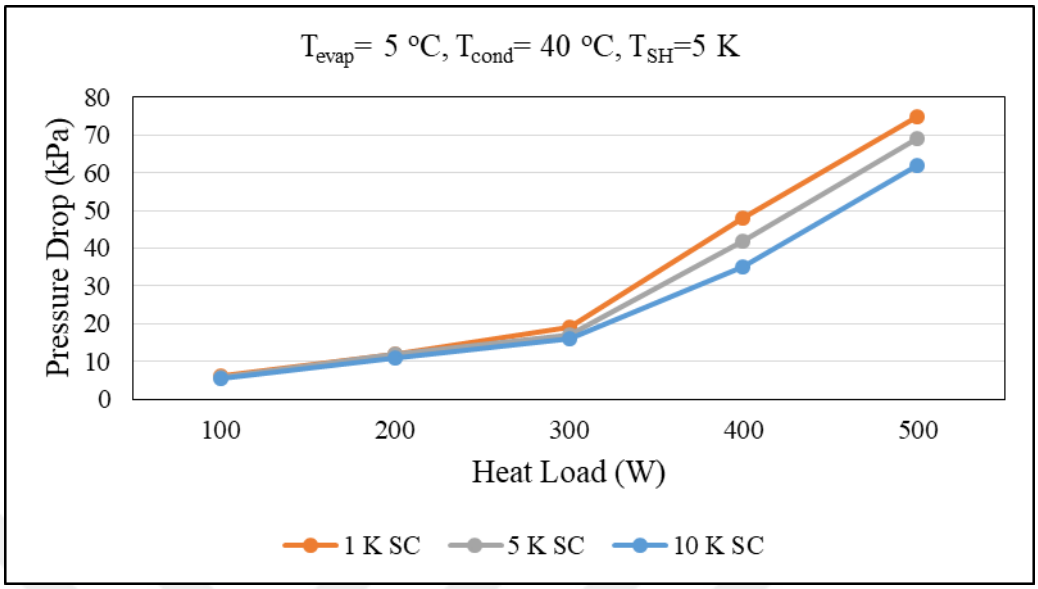

Figure B1.3: Pressure drop in evaporator 1.

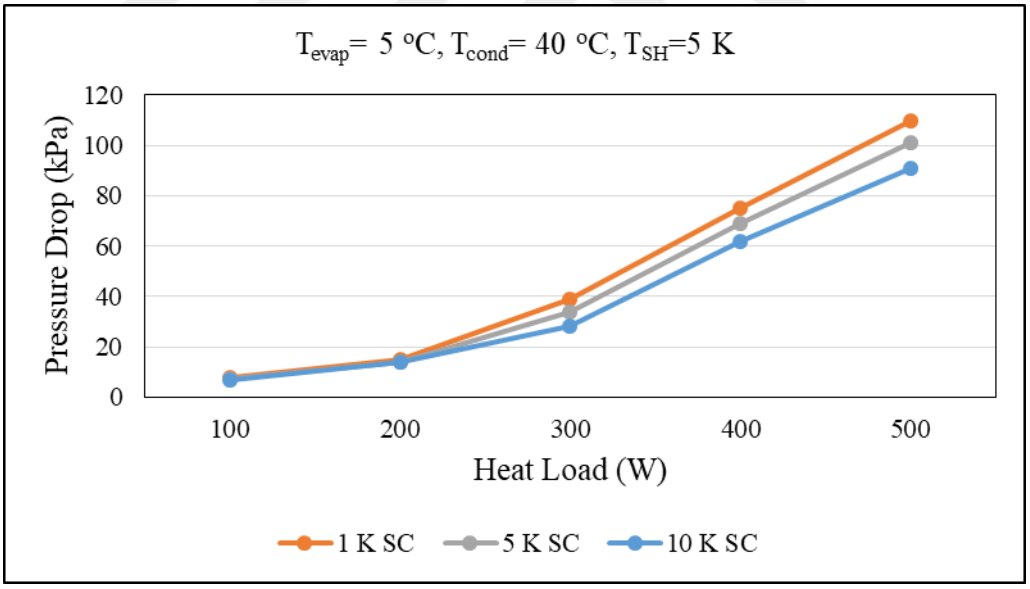

Figure B1.4: Pressure drop in evaporator 2.

- The Effect of Subcooling at 1 K Superheat

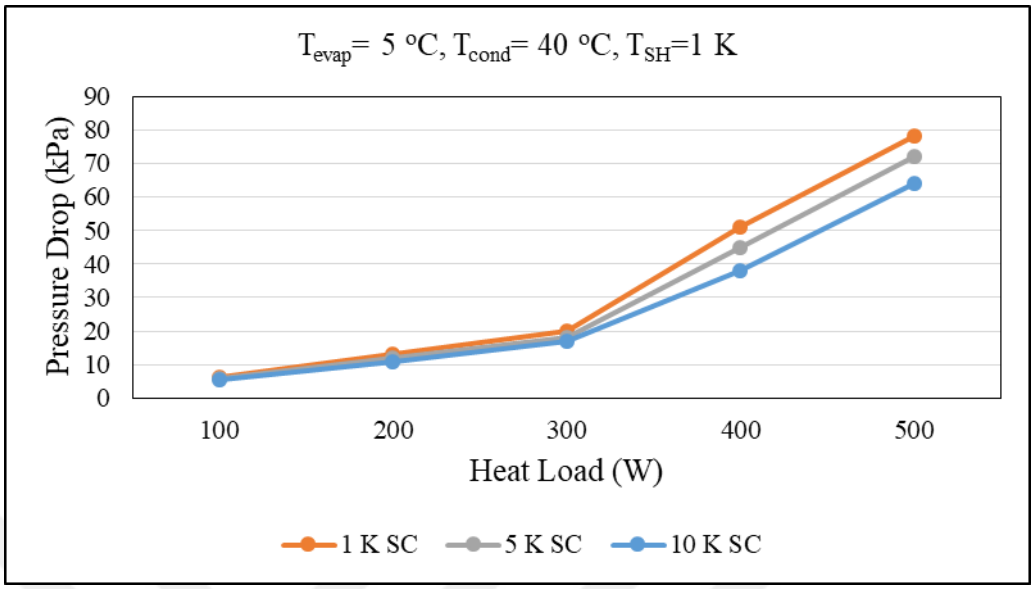

Figure B1.5: Pressure drop in evaporator 1.

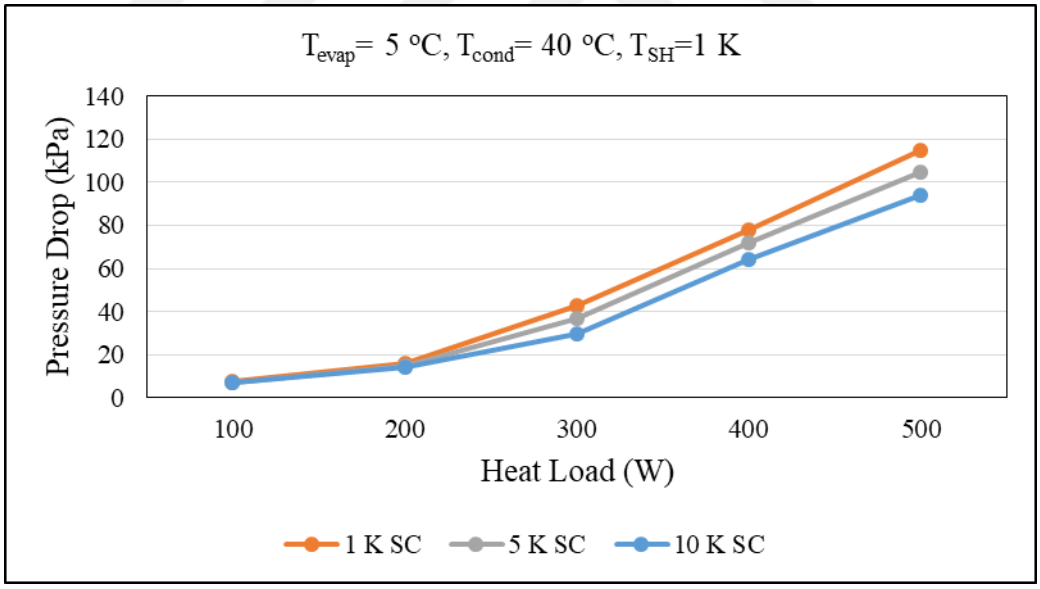

Figure B1.6: Pressure drop in evaporator 2.

Appendix C: The Time Dependent of Temperature Data

Table C1.1: Temperature data.

	Evaporator 1	Evaporator 2	Evaporator 1	Evaporator 2	Evaporator 1	Evaporator 2	Evaporator 1	Evaporator 2	Evaporator 1	Evaporator 2
T	100 W	100 W	200 W	200 W	300 W	300 W	400 W	400 W	500 W	500 W
t1	81,41	87,67	101,84	108,91	121,25	123,56	129,16	130,28	171,83	173,36
t2	80,26	86,83	100,75	107,78	119,76	121,21	126,84	127,82	168,47	165,88
t3	79,03	86,72	97,37	106,65	116,07	118,86	124,54	126,56	162,49	162,70
t4	77,87	86,39	96,27	105,37	112,59	117,69	122,19	124,00	156,99	160,19
t5	76,61	85,86	95,13	104,07	110,14	115,22	119,83	122,75	147,35	157,17
t6	75,43	85,10	93,20	102,74	107,78	111,49	117,41	120,20	145,40	154,58
t7	74,22	84,93	92,33	101,35	105,37	108,94	115,04	118,92	140,54	147,07
t8	73,01	84,88	90,68	99,96	102,74	106,41	112,66	116,29	135,63	144,98
t9	71,78	84,05	85,87	98,58	100,74	103,86	110,17	114,93	130,82	148,11
t10	70,59	83,88	84,61	97,19	99,26	99,87	107,51	112,00	126,00	145,44
t11	69,44	83,55	83,43	95,82	97,76	97,85	105,94	110,69	121,04	142,82
t12	68,39	82,79	81,95	94,40	93,13	95,35	103,01	109,37	118,92	140,20
t13	67,56	81,57	79,06	92,99	89,98	93,97	100,08	108,12	116,29	137,52
t14	66,57	80,29	77,55	91,55	85,27	92,54	97,19	107,06	113,27	134,90
t15	65,41	78,90	76,09	90,09	83,67	91,10	95,58	105,94	110,69	132,27
t16	64,19	77,48	73,11	88,62	82,08	88,11	92,46	105,39	109,37	129,60
t17	62,91	76,04	71,58	87,15	80,48	86,65	90,85	103,84	108,12	126,84
t18	61,63	74,55	70,03	85,68	78,84	85,17	87,66	102,30	105,94	124,02
t19	60,30	73,05	68,50	84,20	77,18	83,67	86,02	100,73	103,01	121,16
t20	59,00	71,59	66,94	82,70	75,51	82,30	84,37	99,16	101,52	120,68